This article is an accepted version. Please cite the published version: https://doi.org/10.1016/j.segan.2025.101801

Journal Pre-proof

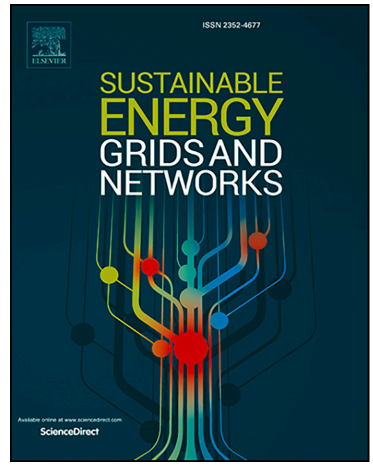

Flexible Robust Optimal Bidding of Renewable Virtual Power Plants in Sequential Markets under Asymmetric Uncertainties

Hadi Nemati, Pedro Sánchez-Martín, Álvaro Ortega, Lukas Sigrist, Enrique Lobato, Luis Rouco

PII: S2352-4677(25)00183-3
DOI: https://doi.org/10.1016/j.segan.2025.101801
Reference: SEGAN 101801

To appear in: *Sustainable Energy, Grids and Networks*

Received Date: 26 June 2024
Revised Date: 5 December 2024
Accepted Date: 14 July 2025

Please cite this article as: Nemati H, Sánchez-Martín P, Ortega ´, Sigrist L, Lobato E, Rouco L, Flexible Robust Optimal Bidding of Renewable Virtual Power Plants in Sequential Markets under Asymmetric Uncertainties, *Sustainable Energy, Grids and Networks* (2025), doi: https://doi.org/10.1016/j.segan.2025.101801.

Flexible Robust Optimal Bidding of Renewable Virtual Power Plants in Sequential Markets under Asymmetric Uncertainties

Hadi Nemati*, Pedro Sánchez-Martín, Álvaro Ortega, Lukas Sigrist, Enrique Lobato, Luis Rouco

Comillas Pontifical University ICAI School of Engineering, Institute for Research in Technology, Madrid, Spain

**Corresponding author*

E-mail address: hnemati@comillas.edu

Abstract

In this paper, a novel approach to define the optimal bidding of Renewable-only Virtual Power Plants (RVPPs) in the day-ahead, secondary reserve, and intra-day markets is proposed. To this aim, a robust optimization algorithm is developed to account for the asymmetric nature of the uncertainties that characterize the market prices, as well as the energy production of the RVPP stochastic sources and flexible demand consumption. Simulation results show increased RVPP benefits compared to other existing solutions and demonstrate the potential of renewable sources to further increase their economic competitiveness. The simplicity of the implementation, the computational efficiency, and the flexible robustness are also verified.

Keywords

Energy markets, renewable-only virtual power plant, reserve markets, robust optimization, stochastic sources.

Nomenclature

Indexes and Sets

$d \in \mathcal{D}$ Set of demands

$k \in \mathcal{K}$ Set of Intra-Day Market (IDM) sessions

$p \in \mathcal{P}$ Set of daily load profiles

$r \in \mathcal{R}$ Set of Non-dispatchable Renewable Energy Sourcess (ND-RESs)

$t \in \mathcal{T}/\mathrm{t} \geq \tau$ Set of time periods/IDM time periods

$\theta \in \Theta$ Set of Solar Thermal Units (STUs)

$\Xi^{\mathrm{DA}}/\Xi^{\mathrm{ID}}_{k}/\Xi^{\mathrm{SR}}$ Set of decision variables of Day Ahead Market (DAM)/IDM#k/Secondary Reserve Market (SRM)

Parameters

$\tilde{P}^{DA}_{r(\theta),t}/\check{P}^{DA}_{r(\theta),t}$ Median/negative deviation of ND-RES r (solar field of STU θ thermal) production in the DAM during period t [MW]

$\tilde{P}^{ID}_{k,r,t}/\check{P}^{ID}_{k,r,t}$ Median/negative deviation of ND-RES r production in the IDM#k during period t [MW]

$\tilde{P}^{SR}_{r,t}/\check{P}^{SR}_{r,t}$ Median/negative deviation of ND-RES r production in the SRM during period t [MW]

$\tilde{P}^{DA}_{d,p,t}/\hat{P}^{DA}_{d,p,t}$ Median/positive deviation of hourly consumption of profile p of demand d in the DAM during period t [MW]

$\underline{R}_d/\bar{R}_d$ Down/up ramp rate of demand d [MW/hour]

$\underline{R}^{SR}_{r(d)}/\bar{R}^{SR}_{r(d)}$ Secondary Reserve (SR) down/up ramp rate of ND-RES r (demand d) [MW/min]

$\underline{E}_d$ Minimum energy consumption of demand d throughout the operation horizon [MWh]

$\underline{P}_\theta/\bar{P}_\theta$ Minimum/maximum power production of STU θ [MW]

$\underline{P}_d/\bar{P}_d$ Minimum/maximum power consumption of demand d [MW]

$\underline{P}_r/\bar{P}_r$ Minimum/maximum power production of ND-RES r [MW]

C^R_r Operation and maintenance costs of ND-RES r [€/MWh]

$C_{d,p}$ Cost of load profile p of demand d [€]

M Big positive value [MW]

T^{SR} Required time for SR action [min]

$\underline{\beta}_{d,t}/\bar{\beta}_{d,t}$ Percentage of down/up flexibility of demand d during period t [%]

$\Gamma^{DA}/\Gamma^{ID}_k$ DAM/IDM#k price uncertainty budget [-]

Γ^{DA}_d Demand d consumption uncertainty budget in the DAM [-]

$\Gamma^{DA}_{r(\theta)}$ ND-RES r (Solar field of STU θ thermal) production uncertainty budget in the DAM [-]

$\Gamma^{SR,\uparrow}/\Gamma^{SR,\downarrow}$ Up/down SRM price uncertainty budget [-]

Δt Duration of periods [hour]

ε Small positive value [MW]

κ User-defined parameter to set the limit of up reserve traded in the SRM as a percentage of total power capacity of RVPP [%]

$\tilde{\lambda}^{\mathrm{DA}}_t/\hat{\lambda}^{\mathrm{DA}}_t/\check{\lambda}^{\mathrm{DA}}_t$ Median and positive/negative deviation of DAM price prediction during period t [€/MWh]

$\tilde{\lambda}^{\mathrm{SR},\downarrow}_t/\hat{\lambda}^{\mathrm{SR},\downarrow}_t/\check{\lambda}^{\mathrm{SR},\downarrow}_t$ Median and positive/negative deviation of down SRM price prediction during period t [€/MW]

$\tilde{\lambda}^{\mathrm{SR},\uparrow}_t/\hat{\lambda}^{\mathrm{SR},\uparrow}_t/\check{\lambda}^{\mathrm{SR},\uparrow}_t$ Median and positive/negative deviation of up SRM price prediction during period t [€/MW]

$\tilde{\lambda}^{\mathrm{ID}}_{k,t}/\hat{\lambda}^{\mathrm{ID}}_{k,t}/\check{\lambda}^{\mathrm{ID}}_{k,t}$ Median and positive/negative deviation of IDM#k price prediction during period t [€/MWh]

ϱ_t Coefficient to calculate the ratio of down-to-up reserve requested by the Transmission System Operator (TSO) during period t [%]

Variables

$p^{DA}_{\theta,t}$ Production of STU θ in the DAM during period t [MW]

$p^{DA}_{d,t}$ Consumption of demand d in the DAM during period t [MW]

$p^{DA}_{r,t}$ Production of ND-RES r in the DAM during period t [MW]

$p^{ID}_{k,\theta,t}$ Production of STU θ in the IDM#k during period t [MW]

$p^{ID}_{k,d,t}$ Consumption of demand d in the IDM#k during period t [MW]

$p^{ID}_{k,r,t}$ Production of ND-RES r in the IDM#k during period t [MW]

$p_t^{DA}/p_{k,t}^{ID}$ Total power traded (positive for selling and negative for buying) by RVPP in the DAM/IDM#k during period t [MW]

$p_{\theta,t}^{SF}$ Thermal power output of the solar field of STU θ during period t [MW]

$r_t^{SR,\uparrow}/r_t^{SR,\downarrow}$ Total up/down SR traded by RVPP during period t [MW]

r_t^{SR} Total SR traded by RVPP for different TSO calls on conditions during period t [MW]

$r_{\theta,t}^{SR}$ SR provided by STU θ for different TSO calls on conditions during period t [MW]

$r_{r(d),t}^{SR,\uparrow}/r_{r(d),t}^{SR,\downarrow}$ Up/down SR provided by ND-RES r (demand d) during period t [MW]

$r_{r(d),t}^{SR}$ SR provided by ND-RES r (demand d) for different TSO calls on conditions during period t [MW]

$y_t^{DA}/y_{k,t}^{ID}$ RVPP energy production affected by DAM/IDM#k price uncertainty during period t [MWh]

$y_{d,t}^{DA}$ Demand d consumption affected by uncertainty during period t [MW]

$y_{r(\theta),t}^{DA}$ ND-RES r (solar field of STU θ thermal) production affected by uncertainty during period t [MW]

$\eta_{d,t}^{DA}$ Dual variable to model the demand d uncertainty during period t [MW]

$\eta_{r(\theta),t}^{DA}$ Dual variable to model the ND-RES r (solar field of STU θ thermal) production uncertainty during period t [MW]

$\eta_t^{DA}/\eta_{k,t}^{ID}$ Dual variable to model the price uncertainty of DAM/IDM#k during period t [€]

$\eta_t^{SR,\uparrow}/\eta_t^{SR,\downarrow}$ Dual variable to model the price uncertainty of up/down SRM during period t [€]

ν^{DA}/ν_k^{ID} Dual variable to model the price uncertainty of DAM/IDM#k [€]

$\nu^{SR,\uparrow}/\nu^{SR,\downarrow}$ Dual variable to model the price uncertainty of up/down SRM [€]

ν_d^{DA} Dual variable to model the demand d uncertainty [MW]

$\nu_{r(\theta)}^{DA}$ Dual variable to model the ND-RES r (solar field of STU θ) production uncertainty [MW]

$\chi_{d,t}^{DA}$ Binary variable that is 1 if demand d robust constraints are active during period t, and 0 otherwise [-]

$\chi_{r(\theta),t}^{DA}$ Binary variable that is 1 if ND-RES r (STU θ) robust constraints are active during period t, and 0 otherwise [-]

$u_{d,p}$ Binary variable that is 1 if profile p of demand d is selected, 0 otherwise [-]

1. Introduction

1.1. Motivation

A Virtual Power Plant (VPP) combines and operates several independent assets in a coordinated manner to provide a flexible and economical solution to utilities that otherwise could not be possible. This combination and coordination can partially mitigate some of the issues related to Non-dispatchable Renewable Energy Sourcess (ND-RESs), such as their inherent variability and relatively small size compared to conventional fossil-fuel plants [1]. In this regard, different organizations have manifested their interest in increasing the performance of an integrated portfolio of Renewable Energy Sources (RESs) to operate together as a Renewable-only VPP (RVPP), capable of providing flexibility and ancillary services to the electricity markets while being competitive against other market participants (see, e.g., [2]).

In order to operate the RVPP in an economically viable manner, it is necessary for the RVPP to participate in different electricity markets to cover its costs and generate profit. The primary source of income for the RVPP comes from its participation in the Day Ahead Market (DAM), where the market operator provides or receives payments based on the amount of energy supplied to/consumed from the network [3, 4].

Additionally, operators have designed distinct Intra-Day Markets (IDMs) mechanisms that allow units to (i) “update” their submitted energy volumes after the DAM has been cleared and (ii) compensate for any unexpected imbalance [5]. In contrast to the energy markets, such as the DAM and IDM, which are overseen by the market operator, the reserve markets are settled by the Transmission System Operator (TSO). The reserve is a margin of power that the power plants are required to include in their generation programs to address unexpected load changes or generation failures. In the event of power imbalances, such as those caused by equipment failures or sudden load increases, the Primary Reserve (PR) is the first one to act, ensuring that the frequency returns to acceptable levels. The PR service is typically not offered on the market due to security concerns. Following PR, Secondary Reserve (SR) or Automatic Frequency Restoration Reserve (aFRR) is activated to restore the frequency and area power interchange to their respective reference values [6]. Unlike PR, this service is suitable for market participation as it allows generating units more time to prepare and deliver the required provision. Therefore, it is essential that researchers and engineers carefully evaluate the participation of the RVPP in different energy and reserve markets.

The main limitation of RVPPs is the wide set of uncertainties that characterize the behavior of the units they comprise. These include the ND-RESs production (from wind speed and solar irradiation), as well as demand consumption patterns. Such uncertainties can significantly affect on the participation of RVPPs in the DAM and/or Ancillary Service Markets (ASMs), such as the Secondary Reserve Market (SRM), and thus on their expected benefits. The RVPP operator thus needs to take advantage of other market mechanisms, such as IDMs, to compensate for any forecast errors. Moreover, the forecasted market prices, used to plan the participation of the RVPP in different markets, are also subject to uncertainties that depend on, e.g., the markets’ time scale and forecast horizon [7]. Therefore, handling simultaneously multiple sources of uncertainty with different variabilities is important for RVPP operators to be competitive compared to other market participants [8, 9].

1.2. Literature Review

Short-term electricity trading usually spans a time window of 24 hours, and different pools take place prior to the power delivery. According to the quantity traded, short-term electricity markets can also be categorized into energy markets, in which the market operator gives/receives payments according to the amount of energy supplied to/consumed from the network, and ASMs, related to the reliability and security of the grid [10]. In the literature, there is a vast body of papers that model the behavior of VPP in the energy markets, which mainly includes DAM and IDM [5, 11–14]. These papers neglect the participation of VPP in ASMs, which can bring more benefit for the VPP. Besides, the uncertainties in both ND-RESs and electricity prices are barely studied together in their optimization models.

Apart from DAM and IDM, ASMs exist, efficiently assigning resources to guarantee a reliable power system operation. Frequency and non-frequency-related ancillary services exist. Most of such markets are based on the availability of certain levels of power reserves (capacities) that were adequately scheduled in advance. The papers [15–19] study the VPP participation in multi-markets, including energy and reserve markets. Although VPP offering in simultaneous energy and reserve markets is implemented in the above papers, the complete formulation for reserve provision of each VPP’s units and associated constraints are simplified. For instance, in energy-limited devices, the real-time use of reserve energy affects the reserve capacity offering. Therefore, a simple assumption of a fraction of energy may not be sufficient. Moreover, the reviewed literature mainly focuses on the simultaneous energy and reserve market clearing or on the initial stage (DAM and reserve) of sequential multi-market offerings. However, the complete sequence of multi-markets, which includes several energy and reserve markets and their interactions, has not been considered.

The operation and planning of power systems, in general, and market participation in particular, are subject to multiple sources of uncertainties [7, 20]. Two main approaches can be generally followed to model market price and stochastic energy production/consumption in optimization problems, namely Stochastic Programming (SP) and Robust Optimization (RO) [21]. In the SP, scenarios are constructed based on the probability distribution of uncertain parameters. The scenarios are then used to configure the optimization problem, in which the final results are assigned according to the probability of the scenarios [21]. In [22], a multi-objective model is implemented for VPP, including wind units, hydroelectric power plants, and thermal units, participation in the continuous IDMs. The uncertainties of hydro inflow forecast, wind generation, and shared order book of VPP compared to other market participants are captured through scenarios by a multi-stage SP model. In [23, 24], a two-stage SP approach is proposed to find the optimal bidding strategy of a VPP in the joint energy and reserve market. The uncertainties of ND-RESs generation, demands, reserve deployment requests, and electricity prices (DAM, Balancing Market (BAM), and spinning reserve market) are captured through a scenario generation method. However, constructing a priori scenarios is not always simple or even accurate enough. Moreover, as the number of scenarios increases, the number of constraints and variables in the optimization problem also grows, resulting in an increase in computational burden. However, some works propose techniques to mitigate this increase in computational burden (e.g., [25, 26]). The paper [25] studies a multi-energy VPP to enhance the resilience of agricultural microgrids, where the Probability Density Function (PDF) of several uncertain parameters are formulated to account for Photovoltaic (PV) and solar thermal uncertainties. In [26], the uncertainties associated with speed and power of integrated wind units are modeled using the PDF of uncertain parameters. While using SP based on the PDF of uncertain parameters can reduce computational time, determining the PDF of these parameters is not feasible in some cases due to the unavailability of exact information.

By contrast, RO establishes a formulation that allows obtaining the values of the decision variables based on adverse realizations of the model parameters. RO has the advantage that the mathematical formulation does not grow in the number of variables and constraints as much as it occurs with SP. However, RO results can be too conservative, although the user may define the level of conservatism by selecting the so-called *uncertainty budget* to alleviate this issue [27]. In [28], the RO problem of a price-taker VPP, including wind power plant, demand, and Energy Storage System (ESS), is proposed in the DAM and BAM. The uncertainties considered include market prices and wind production. In [29], an RO approach is discussed to operate a VPP, including hydro-pumped storage units, thermal units, wind and PV plants, and demand in the energy and reserve markets. Symmetric uncertainties of RESs and demand are considered through confidence bounds (price uncertainty is not considered). The up/down reserve bidding by hydro-pumped storage units and thermal units is modeled in the optimization problem. An iterative algorithm based on solving two Mixed Integer Linear Programming (MILP) problems related to hydro-pumped and thermal units operation is offered to solve the resulting two-stage problem. In [28, 29], the uncertainty budget is set on an hourly basis for each uncertainty in the constraints, which implies the decision from the VPP operator of dozens of parameters per uncertain profile in each market session. An approach requiring far less parameters to be adjusted by the operator would ease the usability and implementation of RO-based bidding approaches.

Apart from SP and RO, interval optimization [30–32] and fuzzy optimization [33, 34] are also employed to address uncertainties. In [30], interval optimization is employed to account for uncertainties in wind-integrated units by considering multiple decision vectors associated with different intervals of the objective function of the problem. The potential risk associated with the solution is mitigated by incorporating the average value and the deviation of the objective function across the specified intervals. The paper [31] examines the short-term electricity market participation of a price-maker VPP by considering wind generation and demand uncertainties using interval optimization. In [32], interval optimization is applied to address uncertainties in the profit of a VPP within a regulated electricity market, while also modeling uncertainties in wind units, solar PVs, and demands as constraints within the interval optimization framework. In [33], a bidding optimization model for VPP participation in the DAM and real-time market is developed, considering the uncertainties associated with RESs. Fuzzy optimization is employed to capture the uncertainties in wind and PV generation. This is achieved by defining fuzzy sets and membership functions for each unit and the objective function, thereby enabling the evaluation of their influence. The paper [34] presents a scheduling model for DAM participation of VPP, addressing uncertainties associated with wind units, PV units, electric vehicles, and demand. The model employs fuzzy satisfaction theory to solve a multi-objective problem, managing system compensation costs, abandoned power costs, and VPP operational income. While interval and fuzzy optimizations are applicable for various problems, they have limitations. The solutions obtained through interval optimization can be overly conservative compared to those from RO, as it does not allow for controlling the level of conservatism. The design of fuzzy sets and membership functions in fuzzy approaches is a complex and subjective process, making results challenging to interpret. Additionally, the computational time of fuzzy and interval optimization can be significant, posing challenges for large-scale problems or real-time applications.

There are more advanced models to capture the uncertain parameters in which the two approaches (SP and RO) are combined or improved. For example, in the Stochastic Adaptive RO (SARO) approach, the problem is defined as a max-min-max problem [35, 36]. The third level allows modeling the corrective actions after uncertain parameters occur. Therefore, compared to a simple RO model, there is more flexibility to counter uncertainties. The main limitation of the SARO approach is that not many stochasticities can be included in the model, as otherwise, the problem can easily become too cumbersome computationally. SARO approaches are best suited for problems where feasibility must be strictly guaranteed in all ranges of uncertainties considered. In the problem that is solved in this paper, it can safely be assumed that not complying with the RVPP optimal bid can be admitted, albeit some penalization may be applied.

Distributed RO (DRO) technique is a powerful tool, especially when uncertainties are centered around the type of density distribution. Its primary strength lies in scenarios where the exact distribution of the uncertainty is unknown, and one needs to optimize against the worst-case distribution within a certain ambiguity set. The papers [37–39] use DRO technique to model the uncertainties of RESs in the DAM. In [40], a DRO approach is proposed to model the bidding problem of a VPP in the DAM and BAM. A Wasserstein ambiguity set is used to deal with both uncertainties of electricity price and wind power generation. It is shown that the proposed DRO approach has better out-of-sample performance compared to the SP problem. In the context of this paper, the parameters of the price density functions are not just assumed to be known but are also derived from historical data, making the application of DRO less pertinent.

The coupling of uncertain parameters, such as the production of ND-RES and electricity prices, becomes another significant factor in the energy market operations, influencing the strategies and decisions of RVPP operator in the electricity markets. In the study presented in this paper, a single-level RO is employed to capture the effect of individual uncertain variables. However, this approach does not fully capture the complex inter-dependencies between these parameters. This is a recognized limitation of single-level RO frameworks compared to multi-level RO [41, 42] and SP approaches [13, 19, 36]. Multi-level RO models offer greater flexibility in capturing the interactions between uncertain parameters in the RVPP bidding problem than single-level models. This advantage arises from the addition of a new optimization level that explicitly represents the behavior of uncertainties, such as electricity prices and energy production and their coupling. In this framework, the objective function of the new level can be designed to identify the worst-case scenario for the profit of the RVPP, rather than focusing solely on energy-related metrics. The research on multi-level models introduces various mathematical methods, including adaptive [41, 42] and stochastic RO [13, 19, 36], to deal with the uncertainties in ND-RES output, electricity prices, and their couplings.

Despite their advanced capabilities, these approaches are confronted with significant challenges, including the complexity of implementation and the rapid growth of problem size as the number of iterations during the solution process increases. These limitations can compromise the scalability and computational feasibility of these approaches, particularly in the context of large-scale problems. Moreover, the stochastic simulation-optimization framework [43] integrates coupled uncertainties using copulas and Monte Carlo methods, allowing a probabilistic comprehension of joint effects. However, RO, as applied in this paper, focuses on worst-case scenarios in a single-level RO model within defined bounds, thereby providing computational efficiency at the expense of detailed coupling representation.

Regardless of the approach applied, a feature that the aforementioned RO-based references in the VPP market participation share is that they consider symmetric distributions of the uncertain profiles. This assumption, which simplifies the problem implementation and input data generation, does not accurately represent the reality of, e.g., solar irradiation or wind speed profiles, nor the different market prices. In particular, the modelling of asymmetric uncertainty on DAM prices allows RO to identify scenarios where buying or selling energy worsens the RVPP objective function. Moreover, regardless of the uncertainty approach applied, the references above consider either conventional (thermal) units and/or fast ESSs (e.g., batteries) as part of the VPP. In other words, the ND-RESs rely on thermal or electrochemical units to improve their reliability. The unique challenges faced by renewable-only RVPPs have not been adequately addressed. Besides, the literature mainly focuses on the first market window (generally the DAM with SRM) due to its larger liquidity. However, how the results of that optimization problem affect subsequent market sessions is not analyzed.

Some works in the literature consider the asymmetric nature of uncertain parameters in the RO problem in power system applications. In [44], an uncertainty set, called forward and backward deviations, is introduced to capture the asymmetric distribution of random variables. The authors subsequently refine the proposed method to identify a tractable solution for stochastic linear optimization problems. In [45], an asymmetric uncertainty set is proposed by considering a limited distributional information. In [46], the asymmetric RO model proposed in [45] is developed for reserve scheduling of a wind unit. The authors utilize dual theory to identify the robust counterpart of the proposed bi-level asymmetric RO model. A linear RO is proposed in [47] by considering asymmetric uncertainty bounds for optimal control of systems. The bounds on uncertain parameters are built for cases when full distributional information is available and the case that only limited distributional information is available. However, to the best of the authors' knowledge, the application of RO with asymmetric uncertainty modeling to single-level optimal bidding of RVPP in sequential markets is limited.

Another method for addressing asymmetric uncertainty is multi-band RO uncertainty modeling, which was first introduced in [48] for wireless network design. The objective of this method is to reduce the conservatism level of RO problem against uncertainty. The main idea of this method is to divide the bound of uncertain parameters to several intervals by considering the probability of each interval according to probability density function of uncertain parameters. In this context, a multi-band uncertainty modeling approach is proposed in [49] for unit commitment problems. This method addresses the limitations of the RO approach regarding the selection of intervals with low probability. The application of multi-band uncertainty modeling in security-constrained unit commitment problem is developed in [50, 51] by considering nodal load uncertainty. The authors of [52] employ multi-band uncertainty modeling for transmission expansion problem, considering renewable sources and demand uncertainties. However, defining multiple new uncertainty budgets into the optimization problem increases problem complexity and hinders the applicability of the proposed method. Furthermore, adding more binary variables to the optimization problem and the need for having knowledge on the distribution of uncertain parameters are other disadvantages of this method.

1.3. Paper Contributions

The contributions of this paper are thus threefold:

- *A single-level robust optimization model tailored for RVPPs to define their optimal bidding in sequential energy and reserve markets:* This model considers the interactions and sequences of different energy and reserve markets, thus being specifically tailored to address the intricacies and challenges posed by sequential markets in the European context. Moreover, the high computational efficiency of the proposed single-level optimization problem allows evaluating, through parametric sensitivity analysis, the impact of choosing different uncertainty budgets for the uncertain parameters in the model, providing the user (e.g., the RVPP operator) with the adequate solution to each market condition. To the authors' knowledge, this type of analysis has not been presented in the context of optimal RVPP bidding.

- *Asymmetric uncertainty on robust optimization:* Existing models for VPP market participation assume symmetric uncertainties, which may not accurately represent the real-world scenarios RVPPs face. The proposed robust model handles the asymmetric behavior of uncertain parameters, providing a more realistic representation. An evaluation of how this asymmetric handling impacts RVPP profit is offered. Such evaluation is compared against previously proposed solutions that consider symmetric uncertainty distributions, showcasing the significant differences between the proposed more realistic approach, and the symmetric approximations. The proposed model is also agnostic with respect to the methodology used to generate the forecasts of the probability distributions of the uncertainties. This flexibility ensures that the proposed model remains relevant and adaptable to a wide range of forecasting methodologies, enhancing its practical applicability.

- *Robustness budget on global scheduling horizons:* Traditional single-level robust optimization models often require defining uncertainty budgets on an hourly basis for each uncertain parameter in the constraints. This process can be cumbersome and less intuitive for RVPP operators, specially as the size of the RVPP increases. The proposed approach simplifies this by allowing operators to define a single robustness budget for each parameter across the entire scheduling horizon (e.g., 24 hours). This innovation reduces the complexity of parameterization and enhances the model's practicality, particularly for real-world applications where operators must frequently update their models to align with market windows.

1.4. Paper Organization

The remainder of the paper is organized as follows. The RVPP bidding in sequential energy and reserve markets is introduced in Section 2. An overview of the proposed flexible robust RVPP bidding optimization is presented in Section 3, whereas the detailed formulation is provided in Section 4. Section 5 discusses simulation results for different case studies. Finally, conclusions are drawn in Section 6.

2. RVPP Bidding in Sequential Energy and Reserve Markets

In this section, the concept of *sequential electricity markets* is introduced, and the bidding strategy of RVPP used in this paper for sequential markets participation is presented. While many system operators opt for joint market clearing, especially in day-ahead and intra-day trading, there exist notable instances and specific segments where a sequential market clearing approach is observed. This is particularly evident in the balancing and reserve markets, where individual countries often manage these aspects separately from the main energy market [21, 53]. This distinction is crucial as the dynamics, rules, and challenges of sequential markets differ from those of joint clearing markets. Further, it is important to distinguish between joint market clearing, joint decision-making for determining optimal bids, and joint bidding. In a sequential market clearing structure, decision-making for determining optimal bids can be made jointly (i.e., different markets can be considered simultaneously at the time of making the optimal decision for the market participant, although such markets are cleared sequentially by the operator). The bids for the different markets can then be submitted jointly or sequentially according to market gate closing times. Hence, the choice is to consider sequentially cleared markets for our RO-based formulation of the bidding model. Figure 1 depicts the Spanish electricity market as an example of a typical market sequence in European countries [54]. The Spanish energy markets include DAM and seven IDMs. The generation units and demands send DAM offers for an upcoming day, including both electricity price and energy, to the Spanish Market Operator (OMIE). Units have opportunities to adjust their DAM energy offers by participating in IDMs. The sequential optimization problems are solved in this paper based on the fact that more accurate forecasts of uncertain parameters could be available as time is closer to the power delivery period.

In addition to energy markets, several reserve markets are run to guarantee the security of the system. The SRM associated with Automatic Generation Control (AGC) is run by the Spanish TSO, Red Eléctrica de España (REE). In this regard, the resources of the up and down-regulation provision for the 24 hours of the operation day are assigned by REE for seven operational zones of the Spanish system. Then, each zone is responsible for providing its promised reserve by clearing the offers from its reserve providers. Note that the electric market design shown in Figure 1 can be adapted, upon some adjustments, to the situation in other European countries.

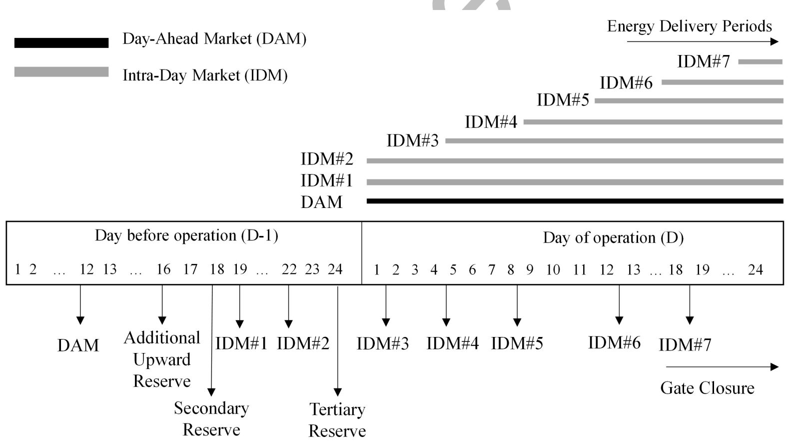

Figure 1: Spanish electricity markets structure [54].

Figure 2 shows the bidding strategy of RVPP in the sequential markets, including DAM, SRM, and IDMs. The information flow between different electricity markets and the necessary input data for running the optimization problems in each of the mentioned electricity markets are also presented. In this paper a price-taker RVPP, i.e., an RVPP with *small size*, is modeled. Therefore, the RVPP does not significantly affect the market clearing price. As market prices are unknown until the market is cleared, the RVPP optimization model considers electricity price forecasts data as inputs, which are generated by means of large sets of historical data. Note that the problem is solved from the RVPP operator point of view as a bidding unit, not from the overall system operator's side. In other words, the RVPP operator does not have access to the bids submitted by other market participants. Therefore, the dual form of the network operation problem is not considered in order to clear the market and to determine the nodal electricity price. Instead, the worst cases of income deviations in the corresponding bounds of electricity price forecast (as well as the forecast bounds of ND-RESs energy and demands) are obtained in the RO problem. Moreover, it is assumed that RVPP bids at zero or low prices. This assumption is relevant since the size of RVPP is small, and it mainly includes ND-RESs with low operation costs. Note that the proposed bidding approach could potentially be adapted for joint clearing markets. For example, if DAM and SRM are cleared at the same time, the RVPP can use the first pane of Figure 2 to bid in these two markets at the same time.

According to Figure 2, the step-by-step solution methodology of the optimization problems for different market sessions in the Spanish electricity market is summarized below:

1. The RVPP receives the input data of its units in addition to the forecast of uncertain parameters before the gate closure of each electricity market selected for participation.

2. The RVPP maximizes its benefits by solving different single-level MILP optimization problems defined in Section 4 related to each market session.

3. The results of solving the optimization problems are used to bid energy or reserve in the corresponding electricity market and to determine the dispatch of RVPP units.

4. The bids submitted by RVPP to the markets are cleared based on the priorities of OMIE and REE, and then the results are sent to the RVPP operator. The energy and reserve bids may or may not be accepted according to the decision of the market operator. Note that the RVPP finds the optimal bids according to the forecast data and whether they are feasible or not will be determined by the system operator.

5. The RVPP uses its accepted bids from previous market sessions as well as the updated input data and forecast of uncertain parameters to solve the optimization problem for the upcoming market session.

Note that in the proposed RVPP bidding scheme, the interconnection between the markets is appropriately addressed. For example, in the case of the DAM objective function, the possibility of providing reserve in the SRM needs to be considered. Therefore, the optimization problem for both DAM and SRM is performed (see upper pane of Figure 2). The RVPP offers energy to the DAM before the DAM gate closure. However, the up/down reserve is not offered and can be reoptimized before the SRM gate closure. In addition, the first IDM (IDM#1) effect in the SRM objective function is considered, but the IDM#1 bid results are not offered in the SRM (see middle pane of Figure 2). Finally, the objective function for each IDM is optimized by considering the bidding results of DAM, SRM, and previous IDMs (see bottom pane of Figure 2). The proposed bidding approach allows the RVPP to omit some of the above electricity markets if so deemed. For instance, the SRM or a number of IDMs can be ignored, and RVPP can go for the subsequent market, in which the input data is based on previously implemented markets. It is worth noting that IDMs are not included in the co-optimization problem of the DAM snapshot. The reason is that the co-optimization of DAM and IDMs can lead to a speculation effect. For instance, a net seller RVPP might attempt to benefit by, e.g., buying a large amount of energy in the DAM to sell it later at a higher price in the IDMs or vice versa. However, this co-optimization is not implemented because usually, the regulator of the system does not allow this kind of participation in the market. Besides, IDMs tend to have much less liquidity than DAM and are mainly used for minor energy adjustments (however, there are some IDM markets with relatively high traded energy such as IDM#1 in the Spanish system). Therefore, with low market liquidity, there is a high risk of not being called in the IDM, thus potentially incurring notable economic losses for the RVPP.

The optimization problems involved in the different electricity markets shown in Figure 2, namely (i) DAM+SRM; (ii) SRM+IDM#1; and (iii) IDM#k, will be developed in Sections 3 and 4 of this paper.

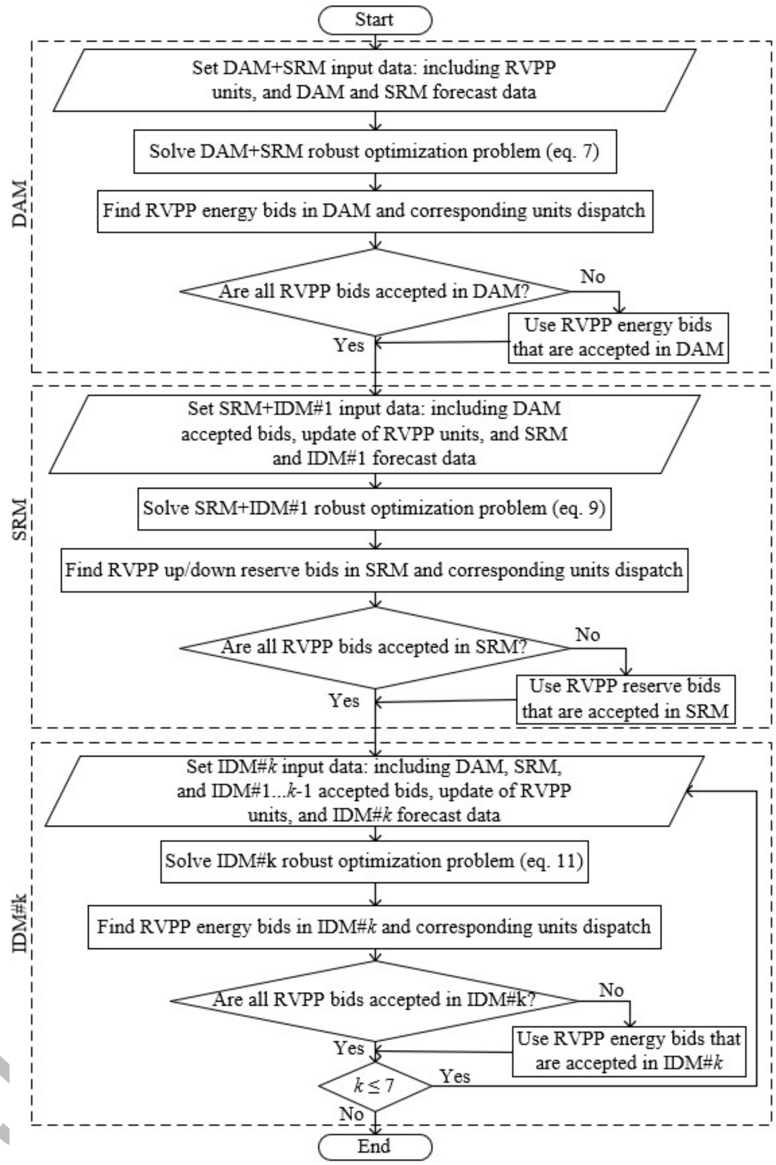

Figure 2: Bidding strategy of RVPP in the sequential electricity markets.

3. Overview of Flexible Robust RVPP Bidding Optimization

The majority of the implementations of flexible RO in VPP applications (e.g., [1, 13, 36, 55]) are based on the principles that Bertsimas and Sim presented in [27]. In the following sections, the approach of Bertsimas and Sim, which is summarized in Appendix A for interested readers, is further developed to consider the asymmetric uncertainty in the objective function and to define the robustness budget on global scheduling horizons of the associated constraints.

3.1. Flexible Robust Optimization of the Objective Function

In this section, the flexible robust formulation of the objective function is formulated by developing the formulation in [27]. For this purpose, consider the following linear deterministic problem:

$$\max \sum_t C_t x_t \tag{1a}$$

st.

$$\boldsymbol{Ax} = \boldsymbol{B}\,, \tag{1b}$$

$$\boldsymbol{C} \leq \boldsymbol{x} \leq \boldsymbol{D}\,, \tag{1c}$$

where C_t is the vector of coefficients of objective function (1a); x_t is the vector of free decision variables; t is the time index representing hours; $\boldsymbol{A}$ and $\boldsymbol{B}$ are matrices of fixed parameters in the equality constraint (1b); $\boldsymbol{C}$ and $\boldsymbol{D}$ are the vectors of lower and upper bounds of inequality constraint (1c), respectively.

To develop the flexible RO on the objective function, let us assume the parameter C_t as a bounded uncertain parameter with the symmetric probability distribution at time t (i.e., $C_t \in [\tilde{C}_t - \check{C}_t, \tilde{C}_t + \hat{C}_t], \check{C}_t = \hat{C}_t$), where $\tilde{C}_t$ is the mean of the uncertain distribution, and $\check{C}_t = \hat{C}_t$ is the deviation at time t. By elaborating on the approach followed in [27] (see Appendix A), (2) is presented as the robust formulation of (1):

$$\max \sum_t \tilde{C}_t x_t - \Gamma^o \nu^o - \sum_t \eta_t^o \tag{2a}$$

st.

$$\nu^o + \eta_t^o \geq \check{C}_t y_t^o\,, \qquad \forall t \tag{2b}$$

$$-y_t^o \leq x_t \leq y_t^o\,, \qquad \forall t \tag{2c}$$

$$\nu^o, \eta_t^o, y_t^o \geq 0\,, \qquad \forall t \tag{2d}$$

$$\boldsymbol{Ax} = \boldsymbol{B}\,, \tag{2e}$$

$$\boldsymbol{C} \leq \boldsymbol{x} \leq \boldsymbol{D}\,, \tag{2f}$$

where Γ^o is a user-defined parameter that represents the robust uncertainty budget in the objective function; ν^o and η_t^o are dual variables related to the parameter uncertainty; and y_t^o is the auxiliary variable of the x_t absolute value function. The first term in (2a) is like the deterministic objective function (1a) by substituting the mean value of uncertain parameter C_t ($\tilde{C}_t$). The second and third terms in (2a) calculate the objective function reduction due to uncertainty of parameter C_t.

In this paper, the asymmetric behavior of uncertain parameters is modeled. To this aim, let us assume the parameter C_t as a bounded uncertain parameter with the asymmetric probability distribution at time t (i.e., $C_t \in [\tilde{C}_t - \check{C}_t, \tilde{C}_t + \hat{C}_t], \check{C}_t \neq \hat{C}_t$), where $\check{C}_t$ is the negative deviation at time t; $\hat{C}_t$ is the positive deviation at time t; and $\tilde{C}_t$ is the median of the distribution (not the mean). To model the asymmetric behavior in the objective function, constraint (2c) is replaced by eq. (3):

$$-\frac{\check{C}_t}{\hat{C}_t} y_t^o \leq x_t \leq y_t^o\,, \qquad \forall t \tag{3}$$

In the above constraint, if $\hat{C}_t = \check{C}_t$, then constraints (2c) and (3) are formally equivalent. Note that although equation (2b) remains unchanged in the asymmetric model, it considers both positive and negative deviations of the uncertain parameter through equation (3). Appendix B provides more information on how the asymmetric robust formulation is obtained, as well as different conditions for the uncertain parameter deviations.

As can be observed from (2), the uncertainty budget is implemented using a parameter Γ^o that adjusts the level of robustness that the user chooses for each source of uncertainty. This uncertainty budget Γ^o represents the number of time periods over the whole scheduling horizon for which an uncertain parameter will take the value that has the worst impact on the objective function. For instance, for a net seller RVPP, prices will take the lowest value in their interval for Γ^o periods in (2), whereas for a net buyer RVPP, the opposite applies.

The uncertainty budget Γ^o can thus take any value between zero (deterministic case without uncertainty – optimistic scenario) and the number of periods of the market horizon, T (pessimistic scenario). For instance, for the DAM, uncertain prices are defined for 24 periods of 1 hour. If Γ^o takes any value between 0 and 24, then the optimization algorithm will choose the Γ^o periods for which the worst realization of the uncertain parameter would impact the most on the objective function. For the remaining $24 - \Gamma^o$ periods, the uncertain parameter would be deterministic, i.e., $C_t = \tilde{C}_t$. If non-integer values for Γ^o are chosen, a fraction of the last period in which uncertainty is included would be considered. With this formulation, the user can select the strategy to follow, either optimistic (low values of Γ^o) or conservative/pessimistic (high values of Γ^o).

3.2. Flexible Robust Optimization of Time-varying Constraints

The uncertainty of stochastic renewable production and demand consumption also needs to be considered in the RVPP optimization problem. However, these uncertain parameters appear in the optimization constraints, which further convolutes the problem and its formulation. To model the flexible robust constraints for stochastic renewable production, let us assume the following deterministic inequality constraint:

$$x_t \leq X_t \,, \qquad \forall t \tag{4}$$

where X_t is the vector of positive upper bounds of inequality constraint (4).

To develop the flexible RO of the sequential constraints for renewable productions, let us assume parameter X_t, which represents the available power production of a given ND-RES, as a bounded uncertain parameter which can take values within the interval $X_t \in [\tilde{X}_t - \check{X}_t, \tilde{X}_t]$, in which $\tilde{X}_t$ is the median of the uncertain distribution, and $\check{X}_t$ is the negative deviation at time t. As uncertainty affects the ND-RES generation, the scenario that has the most negative effect on the objective function is the one in which, for a given period, the uncertain parameter takes the lowest value of its interval, i.e. $X_t = \tilde{X}_t - \check{X}_t$. In the flexible RO framework, the median value of ND-RESs production is selected as the most probable scenario. The worst-case scenarios thus occur when the production of these units lies in the lower 50% of the distribution. Mathematically, this focus on the worst-case scenario is consistent with RO theory, as proved mathematically in [56]. By excluding positive deviations, the computational burden of the problem is also reduced, as the formulation concentrates solely on the most critical deviations affecting the objective function. However, the consideration of positive deviations (abundant production) of ND-RESs might become relevant in alternative modeling approaches. For example, in SP, the entire PDF of uncertain parameters – including both positive and negative deviations – must be modeled, given that each potential realization affects the expected value of the objective function. If, at the scheduled period, there is more energy available than the offered one, the RVPP operator can make use of other market mechanism to leverage the surplus of power/energy, minimizing curtailment. Given the above discussion, the positive deviation of ND-RESs available power, denoted as

$\hat{X}_t$, is not considered in the proposed approach. The opposite applies in the case of flexible demands, i.e., the downward deviation of demand consumption is not considered. By elaborating on the approach followed in [13], the robust formulation (5) is proposed to consider the uncertain parameter X_t in the constraint (4):

$$x_t \leq \tilde{X}_t - y^c_t \,, \qquad \forall t \tag{5a}$$
$$y^c_t \leq \check{X}_t \,, \qquad \forall t \tag{5b}$$
$$y^c_t \geq \nu^c + \eta^c_t - M(1-\chi_t) \,, \qquad \forall t \tag{5c}$$
$$\nu^c + \eta^c_t \geq \check{X}_t \,, \qquad \forall t \tag{5d}$$
$$\varepsilon\chi_t \leq \eta^c_t \leq M\chi_t \,, \qquad \forall t \tag{5e}$$
$$\sum_t \chi_t = \Gamma^c \,, \tag{5f}$$
$$\nu^c, \eta^c_t, y^c_t \,, \qquad \forall t \tag{5g}$$
$$\chi_t \in \{0,1\} \,, \qquad \forall t \tag{5h}$$

where Γ^c is a user-defined parameter that represents the robust uncertainty budget in the optimization constraints; ν^c and η^c_t are dual variables related to the sensitivity of the upper bound value to the robust uncertainty budget; y^c_t represents the negative deviation of the uncertain parameter; ε/M is a small/big positive number; and χ_t is a binary variable that guarantees the robustness budget predefined by the user through Γ^c ($\chi_t = 1$, if for period t the uncertain parameter deviates with respect to the median value).

To develop the flexible robust constraints for demands, parameter X_t is assumed as a bounded uncertain parameter with values within $X_t \in [\tilde{X}_t, \tilde{X}_t + \hat{X}_t]$, in which $\tilde{X}_t$ is the median of the uncertain distribution, and $\hat{X}_t$ is the positive deviation at time t. Then, constraints (5a), (5b), and (5d) are replaced by (6a), (6b), and (6c), respectively:

$$x_t \leq \tilde{X}_t + y^c_t \,, \qquad \forall t \tag{6a}$$
$$y^c_t \leq \hat{X}_t \,, \qquad \forall t \tag{6b}$$
$$\nu^c + \eta^c_t \geq \hat{X}_t \,, \qquad \forall t \tag{6c}$$
$$(5c),\ (5e) - (5h) \,, \qquad \forall t \tag{6d}$$

The set of constraints (5) (and accordingly (6)) needs to be defined for each source of uncertainty in the constraints, i.e., one for each ND-RES and flexible demand unit i that the RVPP contains. This implies that the RVPP operator needs to define as many Γ^c_i as ND-RESs and flexible demands are included in the RVPP. As opposed to price uncertainty budget Γ^o, each Γ^c_i can only take integer values between 0 and the number of periods of each market. This is due to the binary nature of χ_t in (5), which does not allow for non-integer values for Γ^c_i. Implementing a robustness budget on the global scheduling horizons, the higher Γ^c_i is, the more periods in the scheduling horizon include this uncertainty in the model, and thus, the more conservative the solution is. The power deviations of different time periods are chosen based on their magnitude following a decreasing path. That means those time periods that lead to the highest deviation of ND-RES production or demand are chosen before other periods. It is worth mentioning that, in contrast to the proposed model, the literature (e.g., [1, 28]) proposes defining a separate uncertainty budget for each time period of each ND-RES or demand. In the references above, the operator needs to assign substantially more uncertainty budgets for each of the units, which, in most cases, is not an easy task. Besides, it can be inferred that by increasing the value of the uncertain parameter for each time period, the uncertainty evenly affects the objective function instead of selecting the worst scenarios.

Finally, the feasibility of the optimization problem is related to the value of parameter Γ_i^c. For the maximum value of Γ_i^c, the optimization problem is feasible for all possible deviations of uncertain parameters in its predicted bounds. For lower values of Γ_i^c, the optimization problem is feasible for at least the number of worst periods in which energy deviates. The deviation of energy in other periods leads to the probabilistic feasibility of the solution. That means as energy deviates in more time periods with a more considerable amount, the feasibility of the optimization problem decreases.

Note that the RVPP operator bases optimal bid decisions on forecast data, leaving the actual feasibility assessment of these bids (and of other market participants) to the system operator, which is beyond the scope of this paper. In this paper, we introduce in the case studies of Section 5 the concept of *possible unfeasibility* to assess the RVPP's ability to meet market bids considering potential energy fluctuations, since our model optimizes bids within forecast uncertainty limits without pre-judging their feasibility.

The following section builds upon the concepts of RO discussed above, and provides with the detailed formulation proposed in this paper to determine the optimal bidding of RVPPs in sequential energy and reserve markets.

4. Flexible Robust Optimization Model

This section presents and describes the robust formulation of the RVPP bidding problem in the sequential electricity markets, based on the concepts on RO outlined in Section 3. The electricity price uncertainty modeling in the objective function for each DAM+SRM, SRM+IDM#1, and IDM#*k* problem is presented in Section 4.1. Section 4.2 formulates the constraints that do not include any uncertain parameters, such as the supply-demand balancing constraints and the power traded constraints. The uncertainty modeling in the constraints of ND-RES production and flexible demand consumption is discussed in Section 4.3. Finally, the parametrization for different asymmetric uncertainties used in this paper is explained in Section 4.4.

4.1. RVPP Flexible Robust Objective Functions

The objective functions of the three problems illustrated in Figure 2, namely DAM (considering possible SRM participation), SRM (jointly with first IDM session), and IDMs, are presented and discussed in Sections 4.1.1, 4.1.2, and 4.1.3, respectively. Constraints that are associated to such objective functions are also included.

4.1.1. DAM+SRM

The objective function (7) maximizes the benefits of RVPP in the DAM and SRM. The first line of (7) calculates the expected RVPP incomes from bidding in the DAM, up SRM, and down SRM. The parameters $\tilde{\lambda}_t^{DA}$, $\tilde{\lambda}_t^{SR,\uparrow}$, and $\tilde{\lambda}_t^{SR,\downarrow}$ are the median of the uncertain parameters (DAM, up SRM, and down SRM electricity prices) in the objective function. The first line of (7) is analogous to the first term of the objective function (2a) in Section 3.1. The second line depicts the operation costs of ND-RESs and the costs of selecting a particular load profile, and it does not include any uncertain parameter. If single deterministic values are considered for parameters $\tilde{\lambda}_t^{DA}$, $\tilde{\lambda}_t^{SR,\uparrow}$, and $\tilde{\lambda}_t^{SR,\downarrow}$, the first and second lines of (7) behave like the deterministic objective function in the DAM and SRM. In the proposed model, the uncertainty of DAM and SRM prices is considered by finding the worst cases of price deviations in the corresponding forecast bounds. The DAM and SRM price deviations due to uncertainty affect the median income from the first line of the objective function (7). The income reduction due to DAM and SRM price uncertainties is determined by the last two lines of the objective function (7). The last two lines of (7) are the reduction of the total expected incomes of the first line of the objective function (7). They represent the worst realization of the price deviations that consequently has the highest impact on reducing the total benefit of the optimization problem. The last two lines in (7) are analogous to the second and third terms of the objective function (2a). The robust variables ν^{DA}, $\nu^{SR,\uparrow}$, and $\nu^{SR,\downarrow}$ represent the average income reduction per uncertain parameter whose deviation is applied to. The robust variables η_t^{DA}, $\eta_t^{SR,\uparrow}$, and $\eta_t^{SR,\downarrow}$ represent the additional hourly incomes reduction for each price deviation of each market. The uncertainty budgets Γ^{DA} and $\Gamma^{SR,\uparrow}/\Gamma^{SR,\downarrow}$ make the robustness of the model flexible against uncertainties in the DAM and SRM electricity prices, respectively.

$$\begin{aligned}\max_{\Xi^{DA}} & \sum_{t\in\mathcal{T}}\left[\tilde{\lambda}_t^{DA}p_t^{DA}\Delta t+\tilde{\lambda}_t^{SR,\uparrow}r_t^{SR,\uparrow}+\tilde{\lambda}_t^{SR,\downarrow}r_t^{SR,\downarrow}\right]\\ & -\sum_{t\in\mathcal{T}}\sum_{r\in\mathcal{R}}C_r^R p_{r,t}^{DA}\Delta t-\sum_{d\in\mathcal{D}}\sum_{p\in\mathcal{P}}C_{d,p}u_{d,p}\\ & -\Gamma^{DA}\nu^{DA}-\Gamma^{SR,\uparrow}\nu^{SR,\uparrow}-\Gamma^{SR,\downarrow}\nu^{SR,\downarrow}\\ & -\sum_{t\in\mathcal{T}}\left[\eta_t^{DA}+\eta_t^{SR,\uparrow}+\eta_t^{SR,\downarrow}\right]\end{aligned}\tag{7}$$

Constraints (8a) and (8b) model the impact of DAM price volatility on income reduction when electricity price takes its worst condition value by considering price asymmetry. Depending on RVPP selling or buying electricity in the market, the worst DAM price conditions are, respectively, at the prices values $\tilde{\lambda}_t^{DA}-\check{\lambda}_t^{DA}$ or $\tilde{\lambda}_t^{DA}+\hat{\lambda}_t^{DA}$. Constraints (8c) and (8d) calculate the volatility of up and down SRM income reduction when the reserve price takes its worst value, i.e., $\tilde{\lambda}_t^{SR,\uparrow}-\check{\lambda}_t^{SR,\uparrow}$ and $\tilde{\lambda}_t^{SR,\downarrow}-\check{\lambda}_t^{SR,\downarrow}$. The robust formulation selects the hours for price deviation that affect the most (negatively) the incomes of the objective function. As variables $r_t^{SR,\uparrow}$ and $r_t^{SR,\downarrow}$ are positive, there is no need to evaluate the absolute value of these variables. Constraint (8e) defines the nature of positive auxiliary variables. Constraints (8) are written analogous to (2b), (3), and (2d) in Section 3.1, considering three uncertain parameters related to the DAM, up SRM, and down SRM prices.

$$\nu^{DA}+\eta_t^{DA}\geq\check{\lambda}_t^{DA}y_t^{DA}\,,\qquad\forall t\tag{8a}$$

$$-\frac{\check{\lambda}_t^{DA}}{\hat{\lambda}_t^{DA}}y_t^{DA}\leq p_t^{DA}\Delta t\leq y_t^{DA}\,,\qquad\forall t\tag{8b}$$

$$\nu^{SR,\uparrow}+\eta_t^{SR,\uparrow}\geq\check{\lambda}_t^{SR,\uparrow}r_t^{SR,\uparrow}\,,\qquad\forall t\tag{8c}$$

$$\nu^{SR,\downarrow}+\eta_t^{SR,\downarrow}\geq\check{\lambda}_t^{SR,\downarrow}r_t^{SR,\downarrow}\,,\qquad\forall t\tag{8d}$$

$$\nu^{DA},\nu^{SR,\uparrow},\nu^{SR,\downarrow},\eta_t^{DA},\eta_t^{SR,\uparrow},\eta_t^{SR,\downarrow},y_t^{DA}\geq 0\,,\qquad\forall t\tag{8e}$$

4.1.2. SRM + IDM#1

The objective function (9) maximizes the benefits of RVPP in the SRM and IDM#1. The deterministic and robust components of the objective function are distinguishable analogously to Section 4.1.1, considering that the uncertain parameters are related to the up SRM, down SRM, and IDM#1 prices. According to the first line of the objective function (9), before the SRM gate closure, the RVPP maximizes the profits of selling up/down reserve in the SRM and energy in IDM#1. Therefore, the possibility of considering the arbitrage opportunity between SRM and IDM#1 is provided. The second line shows the rescheduled operation costs of ND-RES in IDM#1. The profit reduction due to uncertainties in the SRM and IDM#1 electricity prices are considered through the third and fourth lines of (9).

$$\max_{\Xi^{SR}}\sum_{t\in\mathcal{T}}\left[\tilde{\lambda}_t^{SR,\uparrow}r_t^{SR,\uparrow}+\tilde{\lambda}_t^{SR,\downarrow}r_t^{SR,\downarrow}+\tilde{\lambda}_{(k=1),t}^{ID}p_{(k=1),t}^{ID}\Delta t\right]$$

$$
\begin{aligned}
&- \sum_{t \in \mathcal{T}} \sum_{r \in \mathcal{R}} C_r^R p_{(k=1),r,t}^{ID} \Delta t \\
&- \Gamma^{SR,\uparrow} \nu^{SR,\uparrow} - \Gamma^{SR,\downarrow} \nu^{SR,\downarrow} - \Gamma_{(k=1)}^{ID} \nu_{(k=1)}^{ID} \\
&- \sum_{t \in \mathcal{T}} \left[\eta_t^{SR,\uparrow} + \eta_t^{SR,\downarrow} + \eta_{(k=1),t}^{ID} \right]
\end{aligned} \tag{9}
$$

Constraints (10) set the corresponding benefit reductions of the SRM objective function (9). The first two constraints correspond to the SRM, and the last two constraints to IDM#1. To implement the flexible robustness for IDM#1, the asymmetric price deviation should be the one that sets a resulting price of $\tilde{\lambda}_{(k=1),t}^{ID} - \check{\lambda}_{(k=1),t}^{ID}$ when the RVPP is selling energy to IDM#1 and price of $\tilde{\lambda}_{(k=1),t}^{ID} + \hat{\lambda}_{(k=1),t}^{ID}$ for buying energy. Constraint (10e) defines the nature of positive auxiliary variables.

$$\nu^{SR,\uparrow} + \eta_t^{SR,\uparrow} \geq \check{\lambda}_t^{SR,\uparrow} r_t^{SR,\uparrow} , \qquad \forall t \tag{10a}$$

$$\nu^{SR,\downarrow} + \eta_t^{SR,\downarrow} \geq \check{\lambda}_t^{SR,\downarrow} r_t^{SR,\downarrow} , \qquad \forall t \tag{10b}$$

$$\nu_{(k=1)}^{ID} + \eta_{(k=1),t}^{ID} \geq \check{\lambda}_{(k=1),t}^{ID} y_{(k=1),t}^{ID} , \qquad \forall t \tag{10c}$$

$$-\frac{\check{\lambda}_{(k=1),t}^{ID}}{\hat{\lambda}_{(k=1),t}^{ID}} y_{(k=1),t}^{ID} \leq p_{(k=1),t}^{ID} \Delta t \leq y_{(k=1),t}^{ID} , \qquad \forall t \tag{10d}$$

$$\nu^{SR,\uparrow}, \nu^{SR,\downarrow}, \nu_{(k=1)}^{ID}, \eta_t^{SR,\uparrow}, \eta_t^{SR,\downarrow}, \eta_{(k=1),t}^{ID}, y_{(k=1),t}^{ID} \geq 0 , \qquad \forall t \tag{10e}$$

4.1.3. IDM#k

The objective function of IDM#k participation is provided in (11), where the first term calculates the bidding income in each IDM. The second term computes the rescheduled deterministic operation costs of ND-RES in each IDM. The uncertainties in IDMs electricity prices are captured by the third and fourth terms of (11). The robustness of income reduction in the IDMs objective function (11) comes from IDMs price volatility. The uncertainty budget Γ_k^{ID} should be assigned according to the different number of periods of each IDM session.

$$\max_{\Xi_k^{ID}} \sum_{t \geq \tau} \tilde{\lambda}_{k,t}^{ID} p_{k,t}^{ID} \Delta t - \sum_{t \geq \tau} \sum_{r \in \mathcal{R}} C_r^R p_{k,r,t}^{ID} \Delta t - \Gamma_k^{ID} \nu_k^{ID} - \sum_{t \geq \tau} \eta_{k,t}^{ID} \qquad \forall k \tag{11}$$

Constraints (12) calculate the income reduction arising from the worst case of IDM#k electricity price in the IDM objective function. The price deviations will be those that reduce the expected incomes the most, considering the possible asymmetry in price.

$$\nu_k^{ID} + \eta_{k,t}^{ID} \geq \check{\lambda}_{k,t}^{ID} y_{k,t}^{ID} , \qquad \forall k, t \geq \tau \tag{12a}$$

$$-\frac{\check{\lambda}_{k,t}^{ID}}{\hat{\lambda}_{k,t}^{ID}} y_{k,t}^{ID} \leq p_{k,t}^{ID} \Delta t \leq y_{k,t}^{ID} , \qquad \forall k, t \geq \tau \tag{12b}$$

$$\nu_k^{ID}, \eta_{k,t}^{ID}, y_{k,t}^{ID} \geq 0 , \qquad \forall k, t \geq \tau \tag{12c}$$

4.2. RVPP Deterministic Constraints

This section presents the deterministic constraints to formulate the RO problem for the RVPP market bidding. The supply-demand balancing constraints and the power traded constraints are presented in Sections 4.2.1 and 4.2.2, respectively. In Appendix C, the constraints in this section are developed by considering the internal sub-region network for the RVPP.

4.2.1. Supply-demand Balancing Constraints

The supply-demand balancing constraints for different market problems are presented in this section. Constraint (13) enforces the supply-demand balancing for the RVPP units connected to a single bus, considering both energy and up/down SR in the DAM+SRM. The reserve provision by each of the RVPP units is considered in the power balance constraint (13) by variables $r^{SR}_{r,t}$, $r^{SR}_{\theta,t}$, and $r^{SR}_{d,t}$. Three states are considered for variable r^{SR}_{t}, which is related to the total traded reserve by RVPP. When $r^{SR}_{t} = 0$, the supply-demand balancing constraints are only held for the power. When $r^{SR}_{t} = r^{SR,\uparrow}_{t}$ and $r^{SR}_{r,t} = -r^{SR,\downarrow}_{t}$, the supply-demand balancing constraints are held for the power and up SR reserve and power and down SR, respectively. Similar reserve activation scenarios are defined for units variables $r^{SR}_{r,t}$, $r^{SR}_{\theta,t}$, and $r^{SR}_{d,t}$ according to the above states. The above states keep the power balance equations for all possible SR situations in real-time (i.e., the SR not called on and up or/and down reserve called on). The goal is not to schedule the units according to the actual realization of the reserve, since it is rather difficult to accurately predict the sign and value of the SR activation. However, the logic behind these states is to assign power and SR boundaries (according to delivery time possibilities) to offer the best energy and reserve to the market.

$$\sum_{r\in\mathcal{R}}\left[p^{DA}_{r,t}+r^{SR}_{r,t}\right]+\sum_{\theta\in\Theta}\left[p^{DA}_{\theta,t}+r^{SR}_{\theta,t}\right]=p^{DA}_{t}+r^{SR}_{t}+\sum_{d\in\mathcal{D}}\left[p^{DA}_{d,t}-r^{SR}_{d,t}\right],\qquad\forall t \tag{13}$$

The supply-demand balancing constraint in the DAM+SRM is fairly similar to SRM+IDM#1 and IDM#k problems. If SRM+IDM#1 is solved, the power related to units in the DAM ($p^{DA^*}_{r,t}$, $p^{DA^*}_{\theta,t}$, and $p^{DA^*}_{d,t}$) and the total power traded in the DAM ($p^{DA^*}_{t}$) become parameters, and the variable related to the IDM#1 units power ($p^{ID}_{(k=1),r,t}$, $p^{ID}_{(k=1),\theta,t}$, and $p^{ID}_{(k=1),d,t}$) and total power traded in IDM#1 ($p^{ID}_{(k=1),r,t}$) are added to (14).

$$\begin{aligned}&\sum_{r\in\mathcal{R}}\left[p^{DA^*}_{r,t}+p^{ID}_{(k=1),r,t}+r^{SR}_{r,t}\right]+\sum_{\theta\in\Theta}\left[p^{DA^*}_{\theta,t}+p^{ID}_{(k=1),\theta,t}+r^{SR}_{\theta,t}\right]=\\&p^{DA^*}_{t}+p^{ID}_{(k=1),t}+r^{SR}_{t}+\sum_{d\in\mathcal{D}}\left[p^{DA^*}_{d,t}+p^{ID}_{(k=1),d,t}-r^{SR}_{d,t}\right],\qquad\forall t\end{aligned} \tag{14}$$

In IDM#k, in addition to power related to units in the DAM and the total power traded in the DAM, the reserve provided in the SRM+IDM#1 ($r^{SR^*}_{t}$), the power related to units in the previous IDMs ($p^{ID^*}_{k,r,t}$, $p^{ID^*}_{k,\theta,t}$, and $p^{ID^*}_{k,d,t}$), and the power traded in the previous IDMs ($p^{ID^*}_{k,t}$) become parameters. Besides, the time periods for each session of the IDM#k are updated by substituting (15) instead of (13).

$$\begin{aligned}&\sum_{r\in\mathcal{R}}\left[p^{DA^*}_{r,t}+r^{SR}_{r,t}+\sum_{k=1}^{k-1}p^{ID^*}_{k,r,t}+p^{ID}_{k,r,t}\right]+\sum_{\theta\in\Theta}\left[p^{DA^*}_{\theta,t}+r^{SR}_{\theta,t}+\sum_{k=1}^{k-1}p^{ID^*}_{k,\theta,t}+p^{ID}_{k,\theta,t}\right]=\\&p^{DA^*}_{t}+r^{SR^*}_{t}+\sum_{k=1}^{k-1}p^{ID^*}_{k,t}+p^{ID}_{k,t}+\sum_{d\in\mathcal{D}}\left[p^{DA^*}_{d,t}-r^{SR}_{d,t}+\sum_{k=1}^{k-1}p^{ID^*}_{k,d,t}+p^{ID}_{k,d,t}\right],\qquad\forall k,t\geq\tau\end{aligned} \tag{15}$$

4.2.2. Power Traded Constraints

The power traded constraints for different market snapshots are presented in this section. The equations (16a) and (16b) limit the maximum and minimum power and reserve to be traded in the DAM+SRM. The amount of requested down reserve by the TSO is a proportion of up reserve for each time period, modeled by (16c). Constraint (16d) sets the limit of the up reserve traded in the market according to a share of the total power production capacity of RVPP, defined by the user-defined parameter κ. Note that if $\kappa = 0$, then the RVPP will only participate in the DAM, as no power would be allocated in the SRM.

$$p_t^{DA} + r_t^{SR,\uparrow} \leq \sum_{r\in\mathcal{R}} \bar{P}_r + \sum_{\theta\in\Theta} \bar{P}_\theta \,, \qquad \forall t \tag{16a}$$

$$-\sum_{d\in\mathcal{D}} \bar{P}_d \leq p_t^{DA} - r_t^{SR,\downarrow} \,, \qquad \forall t \tag{16b}$$

$$r_t^{SR,\uparrow} = \varrho_t r_t^{SR,\downarrow} \,, \qquad \forall t \tag{16c}$$

$$r_t^{SR,\uparrow} \leq \kappa \left\{ \sum_{r\in\mathcal{R}} \bar{P}_r + \sum_{\theta\in\Theta} \bar{P}_\theta \right\} , \qquad \forall t \tag{16d}$$

The power traded constraints in the SRM+IDM#1 are written in (17). The power that had already been traded in the DAM is fixed, and the IDM#1 power is added to these constraints.

$$p_t^{DA^*} + p_{(k=1),t}^{ID} + r_t^{SR,\uparrow} \leq \sum_{r\in\mathcal{R}} \bar{P}_r + \sum_{\theta\in\Theta} \bar{P}_\theta \,, \qquad \forall t \tag{17a}$$

$$-\sum_{d\in\mathcal{D}} \bar{P}_d \leq p_t^{DA^*} + p_{(k=1),t}^{ID} - r_t^{SR,\downarrow} \,, \qquad \forall t \tag{17b}$$

$$(16c) - (16d) \,, \qquad \forall t \tag{17c}$$

The power traded in IDM#k is calculated according to (18). The DAM power ($p_t^{DA^*}$), the up and down reserve ($r_t^{SR,\uparrow^*}, r_t^{SR,\downarrow^*}$), and the power related to previous IDMs ($p_{k,t}^{ID^*}$), which had already been assigned in the previous markets, are fixed in these equations.

$$p_t^{DA^*} + \sum_{k=1}^{k-1} p_{k,t}^{ID^*} + p_{k,t}^{ID} + r_t^{SR,\uparrow^*} \leq \sum_{r\in\mathcal{R}} \bar{P}_r + \sum_{\theta\in\Theta} \bar{P}_\theta \,, \qquad \forall k, t \geq \tau \tag{18a}$$

$$-\sum_{d\in\mathcal{D}} \bar{P}_d \leq p_t^{DA^*} + \sum_{k=1}^{k-1} p_{k,t}^{ID^*} + p_{k,t}^{ID} - r_t^{SR,\downarrow^*} \,, \qquad \forall k, t \geq \tau \tag{18b}$$

4.3. RVPP Flexible Robust Constraints

This section presents the robust constraints to formulate the RO problem for RVPP market bidding. With this aim, only the constraints that define the robustness of uncertain RVPP assets, such as ND-RESs, flexible demands, and Solar Thermal Units (STUs), are presented in Sections 4.3.1, 4.3.2, and 4.3.3, respectively. Deterministic operation constraints not modified by the RO (e.g., operation constraints of STUs, etc.) are omitted here. For the sake of conciseness, and without loss of generality, all RVPP units are assumed to be connected to a single bus, and network constraints are thus neglected. The robust constraints proposed in this section can be readily supplemented by network constraints in the form of well-known DC or AC power flow problems. Interested readers can find such constraints in, e.g., [2].

4.3.1. ND-RESs Constraint

The ND-RESs formulation in the DAM and SRM is presented in (19). Constraints (19a) and (19b) limit the up/down reserve that each ND-RES can provide by considering a ramp-constraint response of the

ND-RES and the required time for SR action presented by the TSO. The lower limit of ND-RESs output power is given by (19c). Constraint (19d) is the upper limit of ND-RESs production by considering the median and negative deviation of the power forecast. The median value of ND-RES production is selected as the most likely scenario, while the worst-case scenarios are defined for lower energy production in the RO problem [56]. Therefore, only negative deviations are considered in the formulation to define the worst-case scenarios, as positive deviations will always benefit the RVPP (see also the discussion in Section 3.2). Constraints (19e)-(19k) apply the robust formulation to the uncertain parameters for stochastic ND-RESs generation similar to (5) in Section 3.2. The binary variable $\chi^{DA}_{r,t}$ sets the active or non-active status of each period to satisfy the predefined robustness budget. In this work, Γ^{DA}_r is included in the formulation to make the highest energy reduction scenario in the entire operation horizon flexible, as a robustness budget for a global scheduling horizon. Constraint (19e) assigns the maximum value for power reduction in each period according to the uncertainty budget Γ^{DA}_r that the RVPP operator predefines for the entire operation horizon. The dual variables related to ND-RESs energy uncertainties in (19f), ν^{DA}_r and $\eta^{DA}_{r,t}$, set a lower bound on energy deviation. Both dual variables are bounded by (19g) and logically constrained by (19h) based on the active or non-active status of the periods to comply with the robustness budget. If the robust status of a period is active ($\chi^{DA}_{r,t} = 1$), constraint (19h) leads to a reduction of input energy of ND-RESs on that specific period by allowing a positive amount for $\eta^{DA}_{r,t}$. Constraint (19i) limits the number of periods affected by considering the robust strategy. For instance, if $\Gamma^{DA}_r = 3$, the ND-RES power deviation occurs in 3 hours that results in the worst energy reduction. Finally, the nature of positive auxiliary variables is defined in (19j), whereas constraint (19k) shows the nature of auxiliary binary variables.

$$r^{SR,\uparrow}_{r,t} \leq T^{SR}\bar{R}^{SR}_r\ , \qquad \forall r,t \tag{19a}$$
$$r^{SR,\downarrow}_{r,t} \leq T^{SR}\underline{R}^{SR}_r\ , \qquad \forall r,t \tag{19b}$$
$$\underline{P}_r \leq p^{DA}_{r,t} - r^{SR,\downarrow}_{r,t}\ , \qquad \forall r,t \tag{19c}$$
$$p^{DA}_{r,t} + r^{SR,\uparrow}_{r,t} \leq \tilde{P}^{DA}_{r,t} - y^{DA}_{r,t}\ , \qquad \forall r,t \tag{19d}$$
$$y^{DA}_{r,t} \leq \check{P}^{DA}_{r,t}\ , \qquad \forall r,t \tag{19e}$$
$$y^{DA}_{r,t} \geq \nu^{DA}_r + \eta^{DA}_{r,t} - M(1-\chi^{DA}_{r,t})\ , \qquad \forall r,t \tag{19f}$$
$$\nu^{DA}_r + \eta^{DA}_{r,t} \geq \check{P}^{DA}_{r,t}\ , \qquad \forall r,t \tag{19g}$$
$$\varepsilon\chi^{DA}_{r,t} \leq \eta^{DA}_{r,t} \leq M\chi^{DA}_{r,t}\ , \qquad \forall r,t \tag{19h}$$
$$\sum_t \chi^{DA}_{r,t} = \Gamma^{DA}_r\ , \qquad \forall r \tag{19i}$$
$$\nu^{DA}_r, \eta^{DA}_{r,t}, y^{DA}_{r,t} \geq 0\ , \qquad \forall r,t \tag{19j}$$
$$\chi^{DA}_{r,t} \in \{0,1\}\ , \qquad \forall r,t \tag{19k}$$

The robust formulation of ND-RESs in the SRM+IDM#1 and IDM#k problems is fairly similar to the DAM+SRM. If SRM+IDM#1 is solved, the power traded in the DAM ($p^{DA^*}_{r,t}$) becomes a parameter, and the variable related to the IDM#1 power ($p^{ID}_{(k=1),r,t}$) is added to (19c) and (19d). Besides, the parameters related to the median/negative deviation of the ND-RES r production forecast in the SRM ($\tilde{P}^{SR}_{r,t}/\check{P}^{SR}_{r,t}$) are updated for SRM+IDM#1 by substituting (20b), (20c), and (20d) instead of (19d), (19e), and (19g), respectively.

$$\underline{P}_r \leq p^{DA^*}_{r,t} - r^{SR,\downarrow}_{r,t} + p^{ID}_{(k=1),r,t}\ , \qquad \forall r,t \tag{20a}$$
$$p^{DA^*}_{r,t} + r^{SR,\uparrow}_{r,t} + p^{ID}_{(k=1),r,t} \leq \tilde{P}^{SR}_{r,t} - y^{SR}_{r,t}\ , \qquad \forall r,t \tag{20b}$$

$$y_{r,t}^{SR} \le \check{P}_{r,t}^{SR}\,, \qquad \forall r,t \tag{20c}$$
$$v_{r}^{SR} + \eta_{r,t}^{SR} \ge \check{P}_{r,t}^{SR}\,, \qquad \forall r,t \tag{20d}$$

In IDM#k, in addition to the power traded in the DAM, the power in the previous IDM#1-IDM#$k-1$ ($p_{k,r,t}^{ID^*}$) becomes a parameter. The forecast parameters of ND-RES r production in the IDM ($\tilde{P}_{k,r,t}^{ID}/\check{P}_{k,r,t}^{ID}$) are updated. Besides, the time periods for each session of the IDM#k are updated by substituting (21) instead of (19c), (19d), (19e), and (19g).

$$\underline{P}_r \le p_{r,t}^{DA^*} - r_{r,t}^{SR,\downarrow} + \sum_{k=1}^{k-1} p_{k,r,t}^{ID^*} + p_{k,r,t}^{ID}\,, \qquad \forall k,r,t \ge \tau \tag{21a}$$
$$p_{r,t}^{DA^*} + r_{r,t}^{SR,\uparrow} + \sum_{k=1}^{k-1} p_{k,r,t}^{ID^*} + p_{k,r,t}^{ID} \le \tilde{P}_{k,r,t}^{ID} - y_{k,r,t}^{ID}\,, \qquad \forall k,r,t \ge \tau \tag{21b}$$
$$y_{k,r,t}^{ID} \le \check{P}_{k,r,t}^{ID}\,, \qquad \forall k,r,t \ge \tau \tag{21c}$$
$$v_{k,r}^{ID} + \eta_{k,r,t}^{ID} \ge \check{P}_{k,r,t}^{SR}\,, \qquad \forall k,r,t \ge \tau \tag{21d}$$

4.3.2. Flexible Demands Constraints

The robust constraints associated with the flexible demands are formulated in this section. This formulation builds upon the deterministic model of flexible demands in RVPPs presented in [57]. There, the authors proposed a bi-level flexibility model for demands, where the first level involves selecting a consumption profile from a pre-defined set in the DAM, and the second level defines thresholds around the selected profile to vary consumption in SRM and IDMs.

Constraint (22a) assigns the demand for each period to predefined profiles of demands considering the median and positive deviation of demand. Constraint (22b) assures that only one profile between several profiles of the load is selected by the algorithm. The maximum positive deviation of demand is limited by (22c) and (22d). Constraints (22a)-(22d) are elaborated based on the approach of selecting the predefined profiles of demands in [57] and by applying the robust method analogous to constraints (6a) and (6b) in Section 3.2. Constraints (22e)-(22h) are defined similarly to robust constraints (5c), (6c), (5e), and (5f) in Section 3.2 to assign the maximum value for demand in each period according to the uncertainty budget Γ_d^{DA} which RVPP operator defines. Constraints (22i)-(22l) limit the up/down reserve by a specified amount of load (flexibility of demand) selected by constraint (22a), considering that the uncertainty can affect demand in some periods. The ramp-up and ramp-down limitations of load are restricted by (22m) and (22n), respectively. These constraints define the worst condition of the ramp rate of the load when the up or down reserve is activated in two sequential periods. Constraints (22o) and (22p) bound the load capability for providing the up/down reserve. Constraint (22q) confines the minimum energy that the demand should use. This equation is written for the worst condition of providing reserve from the minimum daily energy consumption perspective, i.e., when the demand provides the up reserve which requires the demand to further reduce its consumption. Finally, constraints (22r) and (22s) define the nature of positive and binary variables, respectively. The robust formulation of flexible demands in the SRM+IDM#1 and IDM#k can be deduced following the same process as for ND-RESs in Section 4.3.1, and their equations are omitted here.

$$p_{d,t}^{DA} = \sum_{p\in\mathcal{P}} \left[\tilde{P}_{d,p,t}^{DA} u_{d,p}\right] + y_{d,t}^{DA}\,, \qquad \forall d,t \tag{22a}$$

$$\sum_{p\in\mathcal{P}} u_{d,p} = 1\,, \qquad \forall d \qquad (22b)$$

$$y^{DA}_{d,t} \le \sum_{p\in\mathcal{P}} \hat{P}^{DA}_{d,p,t} u_{d,p}\,, \qquad \forall d,t \qquad (22c)$$

$$y^{DA}_{d,t} \le M\chi^{DA}_{d,t}\,, \qquad \forall d,t \qquad (22d)$$

$$y^{DA}_{d,t} \ge \nu^{DA}_{d} + \eta^{DA}_{d,t} - M(1-\chi^{DA}_{d,t})\,, \qquad \forall d,t \qquad (22e)$$

$$\nu^{DA}_{d} + \eta^{DA}_{d,t} \ge \sum_{p\in\mathcal{P}} \hat{P}^{DA}_{d,p,t} u_{d,p}\,, \qquad \forall d,t \qquad (22f)$$

$$\varepsilon\chi^{DA}_{d,t} \le \eta^{DA}_{d,t} \le M\chi^{DA}_{d,t}\,, \qquad \forall d,t \qquad (22g)$$

$$\sum_{t} \chi^{DA}_{d,t} = \Gamma^{DA}_{d}\,, \qquad \forall d \qquad (22h)$$

$$r^{SR,\uparrow}_{d,t} \le \underline{\beta}_{d,t}\left(p^{DA}_{d,t} - y^{DA}_{d,t}\right)\,, \qquad \forall d,t \qquad (22i)$$

$$r^{SR,\uparrow}_{d,t} \le p^{DA}_{d,t} - \underline{P}_{d}\,, \qquad \forall d,t \qquad (22j)$$

$$r^{SR,\downarrow}_{d,t} \le \bar{\beta}_{d,t}\left(p^{DA}_{d,t} - y^{DA}_{d,t}\right)\,, \qquad \forall d,t \qquad (22k)$$

$$r^{SR,\downarrow}_{d,t} \le \bar{P}_{d} - p^{DA}_{d,t}\,, \qquad \forall d,t \qquad (22l)$$

$$\left(p^{DA}_{d,t} + r^{SR,\downarrow}_{d,t}\right) - \left(p^{DA}_{d,(t-1)} - r^{SR,\uparrow}_{d,(t-1)}\right) \le \bar{R}_{d}\Delta t\,, \qquad \forall d,t \qquad (22m)$$

$$\left(p^{DA}_{d,(t-1)} + r^{SR,\downarrow}_{d,(t-1)}\right) - \left(p^{DA}_{d,t} - r^{SR,\uparrow}_{d,t}\right) \le \underline{R}_{d}\Delta t\,, \qquad \forall d,t \qquad (22n)$$

$$r^{SR,\uparrow}_{d,t} \le T^{SR}\underline{R}^{SR}_{d}\,, \qquad \forall d,t \qquad (22o)$$

$$r^{SR,\downarrow}_{d,t} \le T^{SR}\bar{R}^{SR}_{d}\,, \qquad \forall d,t \qquad (22p)$$

$$\underline{E}_{d} \le \sum_{t\in\mathcal{T}} \left[p^{DA}_{d,t}\Delta t - r^{SR,\uparrow}_{d,t}\right]\,, \qquad \forall d \qquad (22q)$$

$$\nu^{DA}_{d}, \eta^{DA}_{d,t}, y^{DA}_{d,t} \ge 0\,, \qquad \forall d,t \qquad (22r)$$

$$\chi^{DA}_{d,t} \in \{0,1\}\,, \qquad \forall d,t \qquad (22s)$$

4.3.3. Solar Thermal Units Constraints

STUs are a particular type of ND-RES, as they also include molten-salt energy storage capability, and thus, they cannot be accurately represented by the model in Section 4.3.1. In STUs, the source of uncertainty, i.e., solar irradiation, affects the thermal output power at the solar field, which is then used to either convert it to electric power to be injected into the grid or used to charge the molten-salt storage device. The efficiency of the conversion between thermal and electric powers depends on the thermal power passed through the Power Block of the STU, with typical values of 30-40% (see [58] for more details). The full deterministic model of the STU with its storage can be found in [2, 54]. As justified at the beginning of Section 4.3, only those constraints in the model affected by the robust formulations are presented in (23). Again, the robust formulations of STUs in the SRM+IDM#1 and IDM#k are fairly similar to the DAM+SRM problem, and their equations are omitted.

$$0 \le p^{SF}_{\theta,t} \le \tilde{P}^{DA}_{\theta,t} - y^{DA}_{\theta,t}\,, \qquad \forall \theta,t \qquad (23a)$$

$$y_{\theta,t}^{DA} \leq \check{P}_{\theta,t}^{DA} , \qquad \forall \theta, t \tag{23b}$$

$$y_{\theta,t}^{DA} \geq \nu_{\theta}^{DA} + \eta_{\theta,t}^{DA} - M\left(1 - \chi_{\theta,t}^{DA}\right) , \qquad \forall \theta, t \tag{23c}$$

$$\nu_{\theta}^{DA} + \eta_{\theta,t}^{DA} \geq \check{P}_{\theta,t}^{DA} , \qquad \forall \theta, t \tag{23d}$$

$$\varepsilon\chi_{\theta,t}^{DA} \leq \eta_{\theta,t}^{DA} \leq M\chi_{\theta,t}^{DA} , \qquad \forall \theta, t \tag{23e}$$

$$\sum_{t} \chi_{\theta,t}^{DA} = \Gamma_{\theta}^{DA} , \qquad \forall \theta \tag{23f}$$

$$\nu_{\theta}^{DA}, \eta_{\theta,t}^{DA}, y_{\theta,t}^{DA} \geq 0 , \qquad \forall \theta, t \tag{23g}$$

$$\chi_{\theta,t}^{DA} \in \{0, 1\} , \qquad \forall \theta, t \tag{23h}$$

4.4. Asymmetric Uncertainty Parametrization

Different approaches have been proposed in the literature for quantifying the forecasted bounds of uncertain parameters. Common methods include using historical data [59], fitting parametric distributions [60], and applying bootstrapping techniques [61]. The historical data approach for determining the confidence level of uncertain parameters entails the examination of past data to forecast the values of these parameters. This data, which can be collected from observations, measurements, and historical records, is processed and analyzed to identify patterns and relationships within it. Fitting a parametric distribution to determine the forecast intervals of uncertain parameters requires choosing a suitable distribution, guided by domain expertise and also the properties of the input data. Finally, bootstrapping approaches involve repeatedly sampling from the input data of uncertain parameters to create multiple bootstrap samples. An estimated forecasted bound is then determined by aggregating the results obtained from all these samples.

In this paper, historical data are used to determine the upper and lower bounds of the asymmetric uncertain parameters. The dataset of past observations is analyzed to predict the behavior of the uncertain parameters. The historical data for DAM electricity price [62] and wind energy production [63] over a 30-day workday period are presented in Figures 3 and 4, respectively. The data patterns for each hour are analyzed, with hour 15 as an illustrative example in the figure. Histograms of the historical data, which reveal the asymmetric distributions of the parameters, are generated for each hour across consecutive days. Based on these histograms, the median, mean, 10%, and 90% percentiles are extracted and used as bounds for the RO simulations.

After thoroughly describing the robust RVPP bidding optimization algorithm in (7)-(23) as a manageable, single-level MILP problem, and the parametrization of the uncertainties, several case studies are then explored in Section 5. These case studies have been designed to test and validate the algorithm's efficacy and practical applicability.

5. Case Studies

In this section, a set of case studies is presented to evaluate the proposed flexible RO model for RVPP market bidding. To this aim, different RVPP configurations and electricity market sequences are considered. The RVPP may include a wind farm, a solar PV plant, an STU, and/or flexible demand. A residential aggregator is considered for the flexible demand, with three different profiles available for choice at the DAM, as in [57]. The minimum daily consumption of each profile is 360 MWh. The maximum possible demand value at each period is 30 MW. During SRM and IDMs, the demand owner allows a ±10% tolerance for additional demand flexibility over the selected profile at DAM.

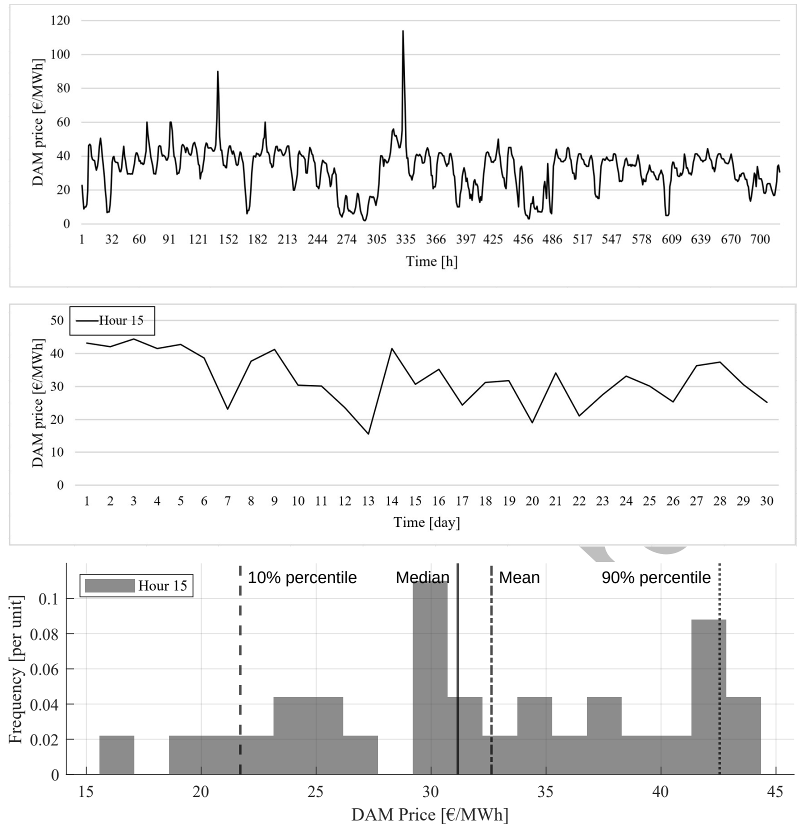

Figure 3: Historical data of DAM electricity price and associated bounds in a specific hour [62]: (a) Historical data for 30 days; (b) Data in hour 15 for 30 days; (c) Histogram in hour 15.

The forecast data of the wind farm and solar PV energy production available to solve the DAM are depicted in Figure 5 [63, 64]. Only negative deviations are evaluated, as discussed in Section 4.3. Updates of such uncertain profiles for subsequent market sessions, as well as for the STU, are defined similarly and not shown here. The solar PV and the wind farm both have a rated capacity of 50 MW each, and their operation costs are respectively 5 €/MWh and 10 €/MWh. The STU power block has a rated electrical capacity of 50 MW, and the thermal storage capacity of the STU is 1100 MWh [58]. The operation cost of the STU is 15 €/MWh. The price forecast data for DAM, SRM, and IDM#1 are adopted from the REE website, and the former is shown in Figure 6 for the sake of illustration [62], where the asymmetric distribution is apparent.

Table 1 shows the RVPP configuration and uncertainty data included in each case study. In *Case 1*, the capability of the proposed model to handle the asymmetric uncertainties in the electricity prices and to consider the whole period for energy robustness compared to the RO formulation proposed in [28] and the SP approach in [1] is evaluated. In *Case 2*, multiple uncertainties in the ND-RESs production, flexible demand, and electricity market prices (DAM & SRM) are considered to show the effectiveness of the proposed model. Besides, the sensitivity analysis for different uncertainty budgets is done to evaluate the behavior of RVPP operator considering risk. In *Case 3*, the bidding strategy of RVPP in the sequential markets is analyzed by considering the updated forecast data in the SRM and IDMs.

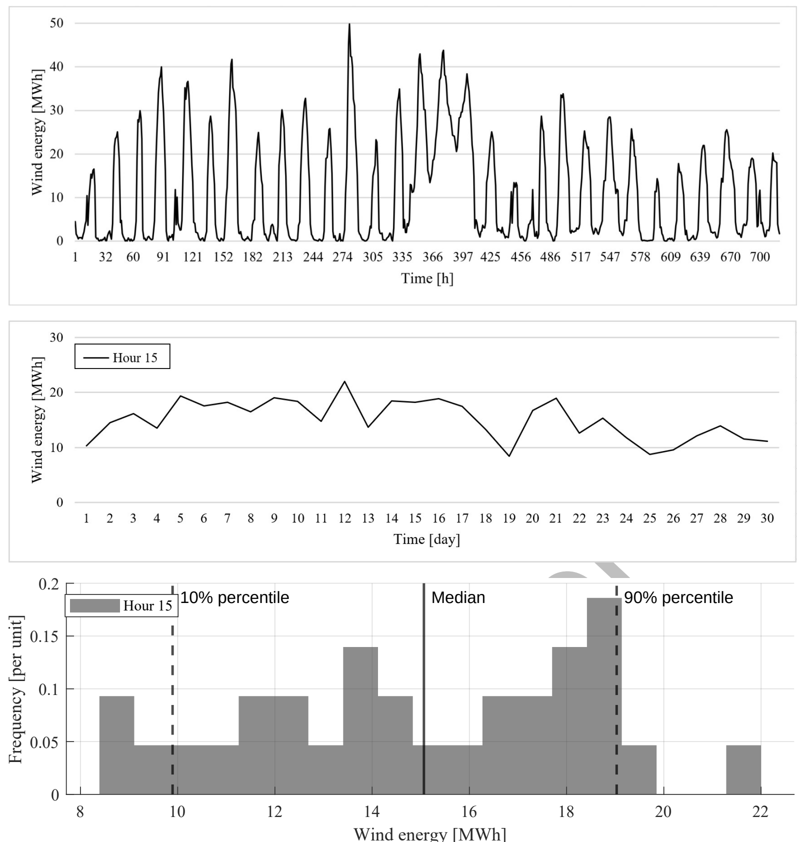

Figure 4: Historical data of wind energy and associated bounds in a specific hour [63]: (a) Historical data for 30 days; (b) Data in hour 15 for 30 days; (c) Histogram in hour 15.

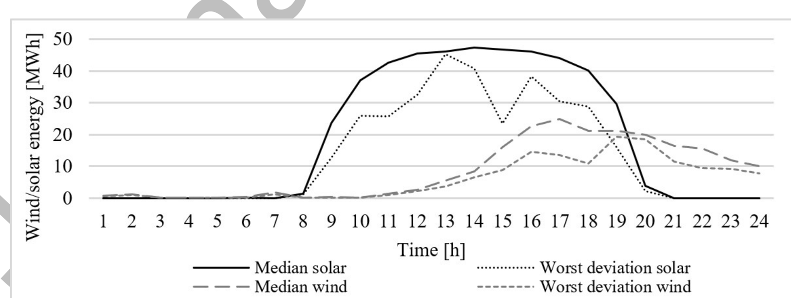

Figure 5: Median/worst case of wind/solar production in the DAM [63, 64].

The simulations are carried out using a Dell XPS with an i7-1165G7 processor, 2.8 GHz, and 16 GB of RAM using the CPLEX solver in GAMS 38.3.0. The simulation time for all case studies in the proposed model is below 2 seconds.

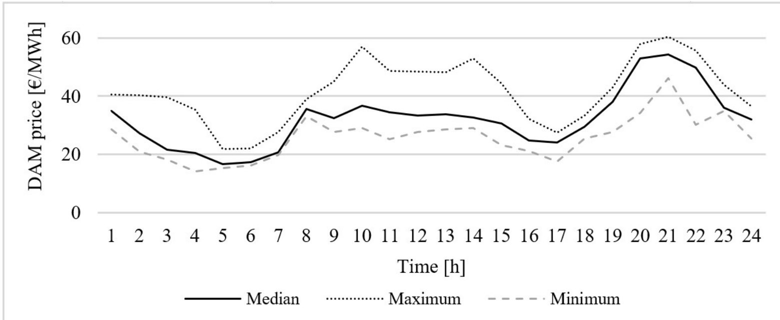

Figure 6: DAM electricity price forecast range [62].

Table 1: RVPP configuration and uncertainty data of each case study.

Case	RVPP configuration				Uncertain data						
	Wind	Solar	STU	Demand	Wind	Solar	STU	Demand	DAM	SRM	IDMs
1	✓	✓	✓	✓	✓	✓	✓		✓	✓	
2	✓	✓	✓	✓	✓	✓	✓	✓	✓	✓	
3	✓	✓		✓	✓	✓			✓	✓	✓

5.1. Case 1

In the first analysis of *Case 1*, only uncertainties in electricity prices are considered. Figure 7 compares the DAM traded power for the proposed model and the model in [28] by considering uncertainties in the DAM and SRM price ($\Gamma^{DA} = 5$ and $\Gamma^{SR,\uparrow}/\Gamma^{SR,\downarrow} = 5$). The figure also depicts the maximum and minimum deviation of the DAM price forecast compared to the median and mean values. Figure 8 presents and compares the traded up/down reserve, as well as the SRM price and its deviation. In [28], the asymmetry in the electricity prices is not considered, so instead of the median value of forecast data, the mean value is used in the objective function of the optimization problem. Considering different electricity prices leads to some differences between the results of both models. The proposed model results in more conservative results in hours 10, 12, 13, and 14; therefore, the RVPP sells less energy in the electricity market. For instance, the traded energy in hours 10 and 14 is 22% and 40% lower than the model proposed in [28]. However, the proposed model results in selling more energy in the DAM in hours 11, 16, 17, and 22. In hour 17, the sold energy in the model proposed in [28] is 40% lower than the proposed model. These differences between traded energy in both models are due to the variation of electricity prices that in turn comes from uncertainty occurring in different hours. Therefore, considering lower electricity prices in hour 17 in the model proposed in [28] due to uncertainty (the minimum electricity price), the STU in the RVPP stores energy in this hour to provide more up reserve in hour 22 according to Figure 8.

Figure 9 compares the DAM profit in the proposed model and the model in [28] for different combinations and values of uncertainty budgets. These include the *energy robustness case* (wind and solar production), the DAM *price robustness case*, and the *price-energy robustness case*. The energy uncertainty budget in the proposed model ($\Gamma^{DA}_{r(\theta)}$) and the model in [28] ($\Gamma^{DA}_{r(\theta),t}$) changes between 0-24 and 0-1, respectively. Therefore, the uncertainty budget is shown in relative terms with respect to the maximum budget. Price uncertainty budgets for both models (Γ^{DA}) are similar and change between 0-24. The figure shows the

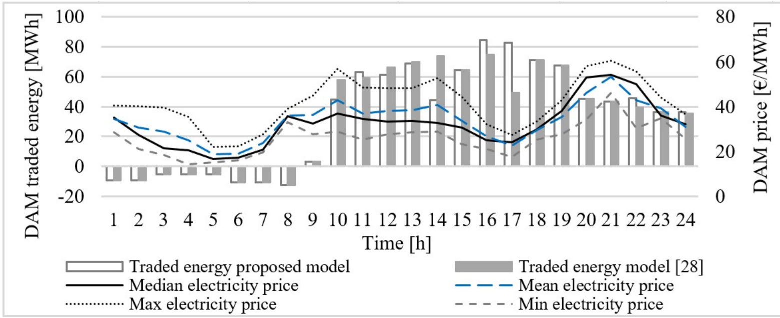

Figure 7: DAM electricity price forecast range and traded power in *Case 1* for the proposed model and the model in [28] (Γ^{DA} = 5 and $\Gamma^{SR,\uparrow}/\Gamma^{SR,\downarrow}$ = 5).

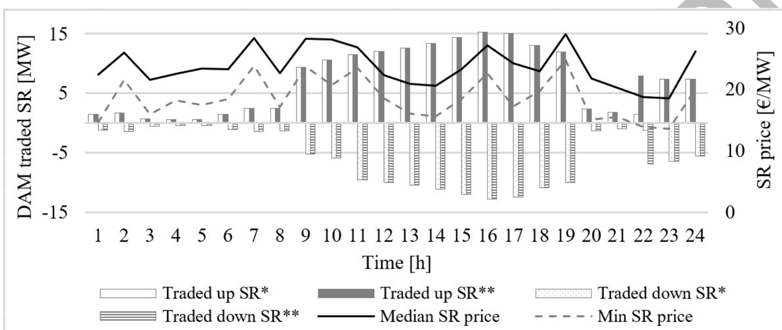

Figure 8: SRM price forecast range and traded SR in *Case 1* for the proposed model (*) and the model in [28] (**) in DAM (Γ^{DA} = 5 and $\Gamma^{SR,\uparrow}/\Gamma^{SR,\downarrow}$ = 5).

trend of DAM profit with changes in the uncertainty budget parameters to better illustrate how the worst-case scenarios are captured in each model. The results in the figure show that the proposed model has a superior capability to capture worst-case scenarios than model [28]. The results also indicate that, in the proposed model, the worst cases, i.e., those with the greatest impact on the objective function, are addressed first. In contrast, in the model in [28], the profit is evenly reduced, demonstrating that this model does not effectively distinguish the worst-case scenarios for *price, energy*, and *price-energy robustness cases*. In both models, increasing the uncertainty budget decreases the DAM profit for the above three cases. However, in the proposed model, the saturation of RVPP profit occurs at smaller percentages of uncertainty budget, i.e., worst realizations are captured first. For example, for an uncertainty budget of 21% for the *price robustness case*, the RVPP profit compared to the deterministic case is reduced by 19% and 13% in the proposed model and the model [28], respectively. Besides, the figure shows that in the model [28], the *energy robustness case* is linear, and *price* and *price-energy cases* are almost linear. This is due to the fact that by increasing the energy uncertainty budget, which has a significant effect compared to the price uncertainty budget on RVPP profit, the energy is reduced evenly in all time periods.

It is worth noting that the higher DAM profit observed in the model [28] should not be interpreted as evidence that it is a better approach. The different DAM profits are due to the use of different values of the uncertain parameter as the basis for each RO. For example, in the proposed model, the median DAM electricity price is considered, while the mean DAM price is used in model [28]. This is also a result of using a less conservative approach to capture the uncertainty that leads to higher DAM profit. Moreover, although the results for DAM profit for the proposed model lead to more conservative solutions and, consequently, lower profit for DAM market participation, the penalization cost in the proposed model is significantly lower than that of the model in [28]. This is due to the fact that a more realistic approach is used to model the uncertain parameters (taking into account the asymmetry and considering the uncertainty budget over the entire scheduling horizon) than in the model [28]. This is further illustrated by the out-of-sample assessment performed in the last analysis of *Case 1*.

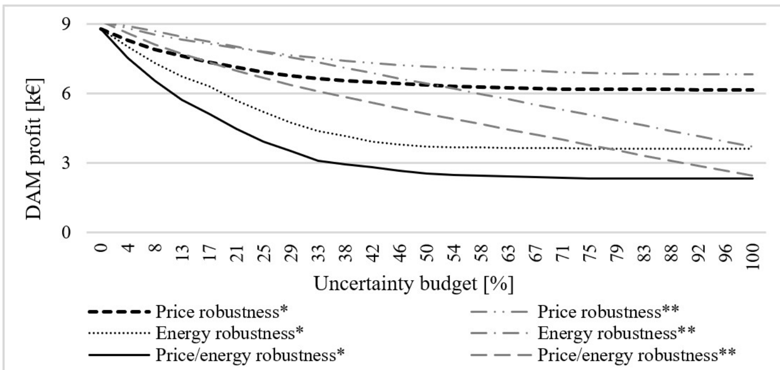

Figure 9: DAM profit in *Case 1* for the proposed model (*) and the model in [28] (**) for various uncertainty budgets: ***Energy robustness:*** ($\Gamma^{DA}_{r(\theta)} \in [0-24]$ or $\Gamma^{DA}_{r(\theta),t} \in [0-1], \Gamma^{DA} = 0$); ***Price robustness:*** ($\Gamma^{DA}_{r(\theta)} = 0$ or $\Gamma^{DA}_{r(\theta),t} = 0, \Gamma^{DA} \in [0-24]$); ***Price-energy robustness:*** ($\Gamma^{DA}_{r(\theta)} = [0-24]$ or $\Gamma^{DA}_{r(\theta),t} = [0-1], \Gamma^{DA} = [0-24]$).

In the second analysis of *Case 1*, only uncertainties in units' energy are considered. Figure 10 compares the possible unfeasible region of wind farm available energy in the deterministic (optimistic) case, in the proposed model for $\Gamma^{DA}_{r} = 5$, and in the model [28] for $\Gamma^{DA}_{r,t} = 5/24$. The possible unfeasible region corresponds to the area between the traded energy and the minimum available energy. These unfeasible regions are depicted using different backgrounds in the figure. By assuming an accurate forecast bound for wind production, unfeasibility can occur if the wind production is less than the median wind production minus the deviation value. In the deterministic case, a relatively large possible unfeasible region is observable according to Figure 10 since any negative deviation during the scheduling period can lead to unfeasibility or penalty for RVPP. In the proposed model, the possible unfeasible region is significantly reduced by capturing the worst case of wind deviation instead of considering even fluctuation.

Finally, in the last analysis of *Case 1*, the uncertainties in both energy and electricity prices are considered. An out-of-sample assessment is performed according to Appendix D to further justify the proposed flexible RO model compared to the symmetric RO model in [28] and SP model in [1]. To ensure a fair comparison between the proposed model and model [28], distinct sets of data are employed for the models and for the out-of-sample assessment. The uncertainty bounds (including upper and lower bounds, mean, and median) for the proposed model and model [28] are assigned in accordance with the explanation provided in Section 4.4. It is worth noting that the uncertainty bounds used for the RO models are not based on the fitting distribution; rather, they are derived from historical data. Besides, to ensure a fair comparison between SP model [1] and the RO models, a different set of scenarios for different uncertainties for SP model [1] are generated by fitting a Weibull distribution to the same historical dataset used to determine the bounds of the proposed model and the RO model [28]. For the out-of-sample assessment, 100 scenarios are generated using Monte Carlo sampling based on the hourly distributions of various uncertain parameters. Note that,

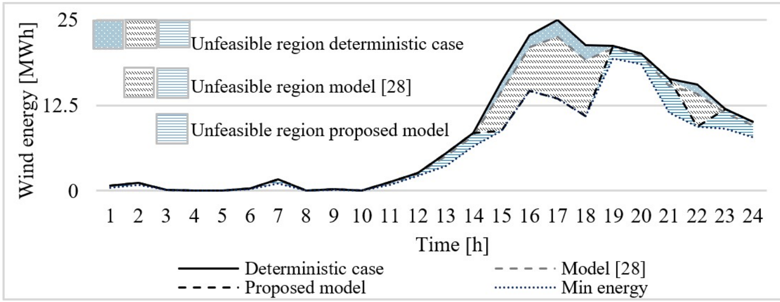

Figure 10: Possible unfeasible region of wind farm energy in *Case 1* in the deterministic model, proposed model ($\Gamma_r^{DA} = 5$) and the model in [28] ($\Gamma_{r,t}^{DA} = 5/24$).

for a fair comparison between the proposed model and models in [1, 28], the same set of scenarios is used for out-of-sample assessment to ensure that the same randomness (or uncertainty) is introduced across both methods. To better capture the asymmetric behavior of different distributions, the Weibull distribution is used to generate the scenarios. The Weibull distribution is a versatile probability distribution capable of modeling various data with varying degrees of skewness and tail behavior. These characteristics make it a valuable tool in statistical analyses. Further details on the fitting distributions to historical data for the out-of-sample assessment and SP model [1] can be found in Appendix E. The parameter Z is a cost coefficient that penalizes the energy infeasibility level in the out-of-sample assessment [19, 36]. The penalty parameter Z is set to 1000 €/MWh similar to [36], in which their authors are similar to [28], to compare better the results of the proposed model and model [28]. In the context of RVPP operation, assigning a high value to this parameter relative to the DAM price is essential to effectively identify infeasible solutions. This ensures that infeasible solutions are correctly identified during the out-of-sample evaluation, as the objective function values for infeasible solutions differ significantly from those of feasible ones.

The results of out-of-sample assessment for different uncertainty budgets are provided in Table 2. Given the dissimilar types of input parameters used in the RO and SP models (e.g., the uncertainty budget in the RO model, which is inapplicable in SP), a separate Table 3 is provided to present the results of the out-of-sample assessment for the SP model [1]. The results compare the average operating profit Π^{av} (excluding the penalization cost), the average penalization cost K^{av}, and the average net profit $\Pi^{av} - K^{av}$ of RVPP. The average operating profit Π^{av} represents the profit of the RVPP from the DAM energy and SRM reserve participation, minus the operation and demand costs in the out-of-sample assessment. The average penalization cost K^{av} accounts for the cost incurred due to not providing some or all of the energy bid in the market. Due to the limited number of hours with renewable production and the low probability of having more than 6 simultaneous hours out of 24 hours at the worst deviation, the table only presents the results for the uncertainty budget between 0-6. The results show that the average penalization cost is very high for the deterministic approach (when all uncertainty budgets are zero). This leads to a significant loss for RVPP according to the first row of Table 2. The model [28] obtains more average operating profit at higher uncertainty budget values than the proposed model. This is due to the fact that the proposed approach is more conservative in capturing the worst-case scenarios. Besides, increasing the uncertainty budget reduces the value of the average penalization cost in both the proposed model and the model [28]. However, considering the worst case of energy uncertainty, the proposed model has a better performance in terms of net profit and average penalization cost. It is worth noting that higher penalizations on some electric markets, such as the SRM, could lead the RVPP to be excluded from participation in those markets. The proposed approach results in higher net profit for all uncertainty budgets (1-6). The net profit in the proposed model is 27.0%, 57.1%, 65.4%, 64.3%, 61.9%, and 74.2% higher than the net profit in model [28].

The results for the SP model [1] in Table 3 demonstrate that as the number of scenarios increases, the operating profit of the RVPP declines gradually due to the inclusion of a broader range of scenarios. The results also indicate that the net profit of the RVPP increases with a higher number of scenarios, as the model becomes more effective at capturing uncertainty. Among the tested scenarios, the use of 60 scenarios yields the highest net profit for the RVPP, but it also imposes a significant computational burden compared to RO models (which is less than 2 seconds for all cases). It is therefore essential to strike a balance between the computational complexity of the model and the resulting net profit when applying the SP approach. In comparison to the RO models (see Tables 2 and 3), the SP approach [1] results in lower changes in both operating profit and net profit. This is due to the fact that the SP approach accounts for all scenarios of uncertain parameters along with their associated probabilities. In contrast, the results of the proposed RO model and the RO model in [28] exhibit higher volatility in these parameters. This is due to the fact that the RO models focus on worst-case scenarios and do not consider the probabilities of these scenarios, making it indifferent to their likelihood. Consequently, the hours that lead to high penalty costs are managed first, regardless of the their probability.

Table 2: The out-of-sample assessment for the proposed model and the model in [28] ($\Gamma^{DA} = \Gamma^{SR,\uparrow} = \Gamma^{SR,\downarrow} = [0-6], \Gamma^{DA}_{r(\theta)} = [0-6]$ or $\Gamma^{DA}_{r(\theta),t} = [0-0.25]$).

	Proposed model			**Model [28]**		
Uncertainty budget [-]	Π^{av} [k€]	K^{av} [k€]	$\Pi^{av} - K^{av}$ [k€]	Π^{av} [k€]	K^{av} [k€]	$\Pi^{av} - K^{av}$ [k€]
0	27.4	215.7	-188.3	27.4	215.9	-188.5
1	24.1	146.1	-122.0	26.4	193.6	-167.2
2	21.3	105.7	-62.5	25.4	171.3	-145.9
3	18.8	62.5	-43.7	24.3	150.7	-126.4
4	16.7	56.9	-40.2	23.4	136.1	-112.7
5	14.8	50.0	-35.2	22.1	114.6	-92.5
6	13.0	34.7	-21.7	21.3	105.7	-84.4

To further verify the results obtained in Table 2, the frequency histograms of defined variables for each scenario and uncertainty budget 2 are depicted in Figures 11, 12, 13. Figure 11 shows the distribution of operating profit of RVPP without considering the penalization cost. Figures 12 and 13 show the distribution of penalization cost and net profit, respectively. The operating profit in the model [28] is more than the proposed model in most scenarios according to Figure 11. However, according to Figures 12 and 13, the proposed model has better performance when the penalization cost is considered.

5.2. Case 2

Figure 14 shows the DAM profit when only energy uncertainties (wind and solar production, STU thermal production, and demand) are considered, when only price uncertainties (DAM and SRM) are considered, and when all uncertainties, both in price and energy, are included. The RVPP income reduction at the saturation point, i.e., when all uncertainty budgets are set to 10 compared to total possible income reduction

Table 3: The out-of-sample assessment for the SP model [1].

	Model [1]			
Number of scenarios [-]	Π^{av} [k€]	K^{av} [k€]	$\Pi^{av} - K^{av}$ [k€]	Computational time [s]
10	21.1	107.2	-86.1	9
20	20.7	98.3	-77.6	18
30	20.3	92.8	-72.5	35
40	20.3	93.7	-73.4	126
50	20.5	94.4	-73.9	252
60	20.4	92.1	-71.7	44305

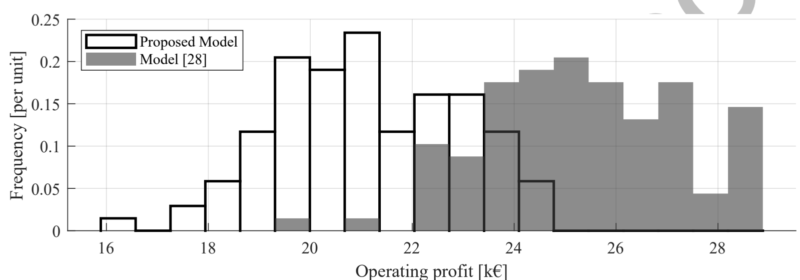

Figure 11: Frequency histogram of sampled daily operating profit for the proposed model and the model in [28] ($\Gamma^{DA} = \Gamma^{SR,\uparrow} = \Gamma^{SR,\downarrow} = 2, \Gamma^{DA}_{r(\theta)} = 2$ or $\Gamma^{DA}_{r(\theta),t} = 2/24$).

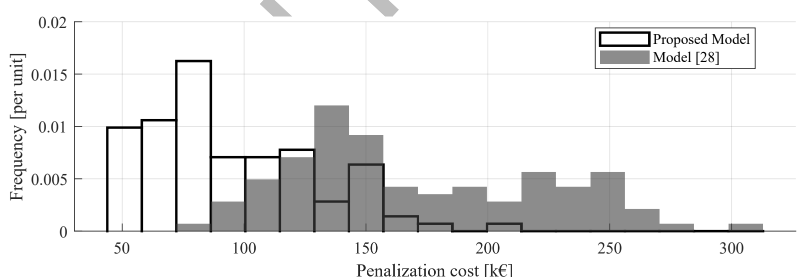

Figure 12: Frequency histogram of sampled daily penalization cost for the proposed model and the model in [28] ($\Gamma^{DA} = \Gamma^{SR,\uparrow} = \Gamma^{SR,\downarrow} = 2, \Gamma^{DA}_{r(\theta)} = 2$ or $\Gamma^{DA}_{r(\theta),t} = 2/24$).

(uncertain parameters=24) for the three cases, *energy robustness*, *price robustness*, and *price-energy robustness*, is 92%, 73%, and 90%, respectively. The larger percentage of income reduction for the *energy robustness case* is due to the fact that the forecasted production of ND-RES and STU units is zero or almost zero in some hours. Therefore, the saturation of income reduction occurs at lower values of uncertainty budget compared to the *price robustness case*. In the *price robustness case*, the DAM and SRM price uncertainty budgets are increased from 0 to 24 in unity steps. By increasing uncertainty budgets, the RVPP income decreases with a higher slope for lower values of uncertainty budgets than for greater ones. This trend is

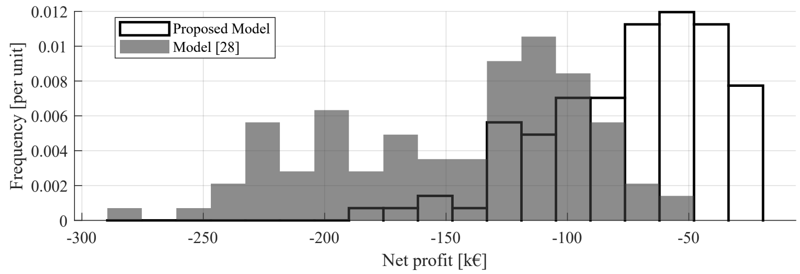

Figure 13: Frequency histogram of sampled daily net profit for the proposed model and the model in [28] ($\Gamma^{DA} = \Gamma^{SR,\uparrow} = \Gamma^{SR,\downarrow} = 2, \Gamma^{DA}_{r(\theta)} = 2$ or $\Gamma^{DA}_{r(\theta),t} = 2/24$).

expected as the worst cases of price deviations are selected first in the robust formulation. Comparing all cases, it can be observed that, in the scenario considered, the majority of the RVPP profit reduction comes from energy uncertainty. Indeed, all RVPP units have uncertain productions, and reducing them has a higher impact on the RVPP income than price fluctuation.

The analysis at the RVPP unit level is next discussed. To this aim, Figure 15 shows DAM traded energy, the wind farm, STU, and solar energy for a deterministic case. Figure 16 depicts the same results as Figure 15 when the uncertainty budgets for energy (wind farm, STU, and solar energy) and electricity price (DAM and SRM) are set to 5. The total sold/bought energy in the uncertain case is decreased/increased by 41% and 8% compared to the deterministic case. By increasing the uncertainty budget, the hours that impose the highest deviations in energy according to the energy forecast are selected as the worst cases. For instance, hours 15-18 and 22 for wind production, hours 11, 12, 15, 17, and 19 for available solar energy, hours 10-14 and 15 for STU available energy, and hours 8, 15-17, and 19 for demand are the worst hours from a deviation perspective for each technology.

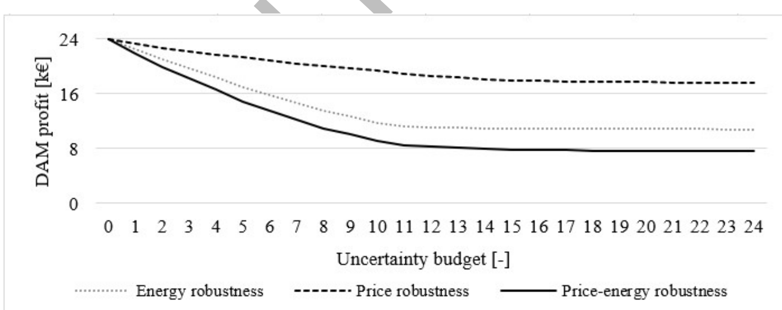

Figure 14: DAM profit in *Case 2* for various uncertainty budgets: **Energy robustness:** ($\Gamma^{DA}_{r(\theta)} = \Gamma^{DA}_{d} \in [0-24], \Gamma^{DA} = \Gamma^{SR,\uparrow} = \Gamma^{SR,\downarrow} = 0$); **Price robustness:** ($\Gamma^{DA}_{r(\theta)} = \Gamma^{DA}_{d} = 0, \Gamma^{DA} = \Gamma^{SR,\uparrow} = \Gamma^{SR,\downarrow} \in [0-24]$); **Price-energy robustness:** ($\Gamma^{DA}_{r(\theta)} = \Gamma^{DA}_{d} = \Gamma^{DA} = \Gamma^{SR,\uparrow} = \Gamma^{SR,\downarrow} \in [0-24]$).

5.3. Case 3

Finally, the flexible robust optimal participation of an RVPP in the complete sequence of market sessions is considered. This case study assumes enough liquidity on IDMs to show the RVPP model capabilities. For instance, the first IDM (IDM#1) in the Spanish market has high liquidity in some circumstances. Figure 17

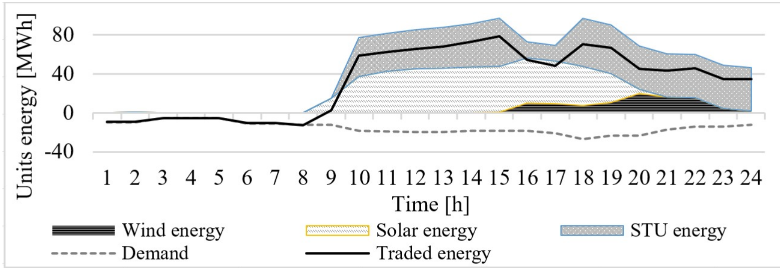

Figure 15: RVPP different units energy and traded energy in *Case 2* in the DAM for deterministic case.

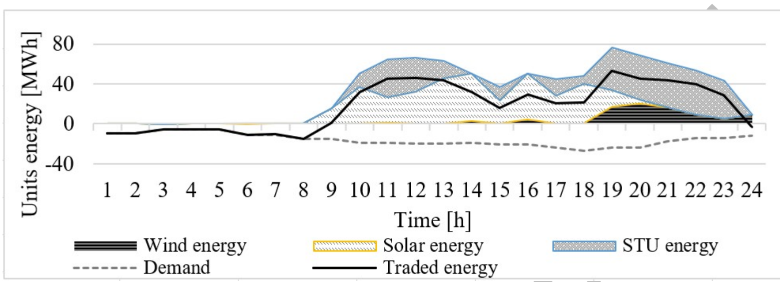

Figure 16: RVPP different units energy and traded energy in *Case 2* in the DAM for $\Gamma^{DA}_{r(\theta)} = \Gamma^{DA} = \Gamma^{SR,\uparrow} = \Gamma^{SR,\downarrow} = 5$.

displays the total traded energy and SR for the deterministic case by assuming RVPP participates in DAM, SRM, IDM#1, and IDM#4. In the deterministic case, RVPP sells most of its available energy in the DAM and IDM#1 between hours 9-22. Besides, the RVPP mostly buys energy in the DAM in hours 1-8 and 23-24. However, the RVPP sells energy in hours 23-24 in IDM#1 to arbitrage energy between DAM and IDM. There is also a small percentage of traded energy in IDM#4 compared to the previous markets, as a small value of energy is usually traded in the last sessions of IDMs. The RVPP trades both up and down SR in the SRM in hours 9-24 as it has available wind or/and solar production.

Figure 18 shows the same results as Figure 17 when the uncertainty budgets for energy (wind and solar) and all price uncertainty budgets are equal to 5. In this case, the RVPP prefers to sell less energy in the DAM due to the uncertainty. In the uncertain case, the total sold/bought energy until the last considered market session (IDM#4) is decreased/increased by 28% and 14% compared to the deterministic case. In hour 15, it sells almost nothing in the DAM and mostly provides the up and down reserve. However, when it goes to IDM#1 with a more precise forecast value, the traded energy in hour 15 is increased. This is also due to the fact that in hour 15, the DAM price is low; however, the IDM price is relatively high, so RVPP has an opportunity to adjust its traded energy. The same trend is understandable for traded energy in IDM#1 compared to DAM between hours 9-19. The amount of trading up and down SR is also decreased compared to the deterministic one as a more conservative strategy is adopted.

6. Conclusion

This paper proposes a novel mathematical formulation of the optimization problem for RVPP participation in sequential energy and reserve markets. A new and efficient flexible RO approach is implemented as an MILP to accurately capture the asymmetric uncertainties in the electricity prices and RESs in the day-ahead, secondary reserve, and intra-day markets. Moreover, as opposed to other RO models, the proposed

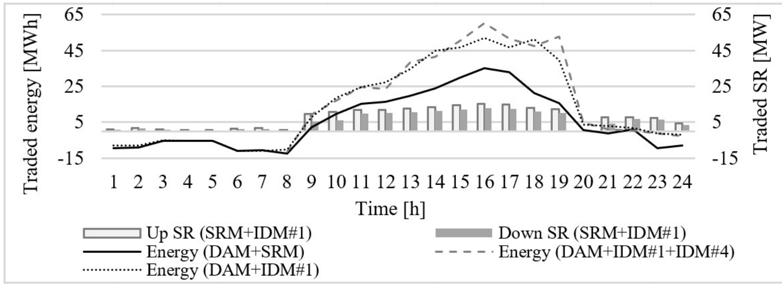

Figure 17: Total traded energy and SR in *Case 3* for deterministic case.

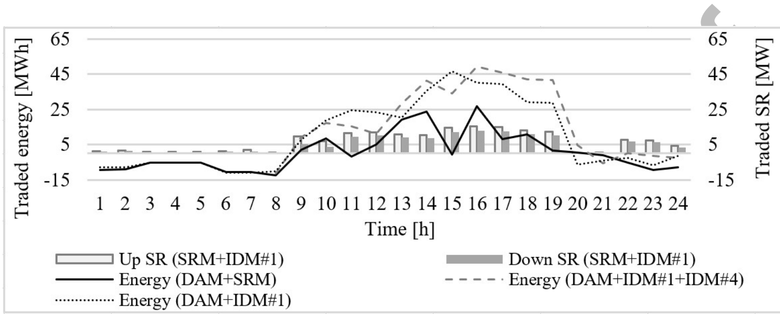

Figure 18: Total traded energy and SR in *Case 3* for $\Gamma_r^{DA} = \Gamma^{DA} = \Gamma^{SR,\uparrow} = \Gamma^{SR,\downarrow} = \Gamma^{ID}_{(k=1)} = \Gamma^{ID}_{(k=4)} = 5$.

approach considers the robustness budget over the whole scheduling horizon, increasing the overall flexibility of the problem, and simplifying the parameter definition of the model. Simulation results show that apart from a more realistic representation of the uncertainties that characterize the problem, the proposed model provides improved results from the feasibility point of view. Moreover, the simplicity and high computational efficiency of the model allow comprehensive evaluations of the results by means of, e.g., parametric sensitivity analyses. Results from such studies indicate that most of the reduction in RVPP profit comes from the ND-RESs energy uncertainty. Moreover, for the cases discussed, considering the uncertainty, the RVPP prefers to trade energy in the IDMs in which the forecast data is more accurate, resulting in less reserve provided. The work presented in this paper can be extended in several ways. On one hand, the optimization problem that has been applied to sequential electricity markets can be formulated for the case of joint electricity market clearing. A probabilistic assessment of the proposed robust model will be provided in future works to determine the required uncertainty budget for each uncertain parameter so that the RVPP operator reaches a certain desired income. Moreover, the benefits of RVPP aggregation will be thoroughly evaluated considering different conditions with respect to the case studies discussed in this paper for model validation and testing. A price-maker optimization model of RVPP as a multi-level problem will be provided to address the increasing penetration of RES in the emerging grids. In this context, the regulatory aspects of the system and the estimated strategies of other market competitors have to be taken into account in the developed model. Moreover, a multi-level problem to identify the worst realizations of the combination of price and energy uncertainties, i.e., incomes robustness, is also under development. In this context, considering the coupling of different uncertain parameters related to ND-RESs and electricity market prices becomes particularly relevant. Finally, extending the current framework to include additional energy sources and their interactions with electricity markets is a valuable direction for future research.

Acknowledgments

This project has received funding from the European Union's Horizon 2020 research and innovation programme under grant agreement No 883985.

Appendix A. Bertsimas and Sim Robust Approach

The robust approach of Bertsimas and Sim [27] is summarized in this appendix, which initially considers the linear optimization problem (A.1).

$$\max \ \boldsymbol{c}^\top \boldsymbol{x} \,, \tag{A.1a}$$

st.

$$\boldsymbol{A}\boldsymbol{x} \le \boldsymbol{b} \,, \tag{A.1b}$$

$$\boldsymbol{l} \le \boldsymbol{x} \le \boldsymbol{u} \,, \tag{A.1c}$$

In (A.1a), $\boldsymbol{x}$ is the vector of free decision variables; $\boldsymbol{c}^\top$ is the transposed vector of fixed parameters of the objective function; $\boldsymbol{A}$ is the matrix of uncertain parameters; a_{ij} are the elements of the matrix $\boldsymbol{A}$; and it is assumed that J_i is the set of elements in row i of the matrix $\boldsymbol{A}$ that are subject to uncertainty. Each entry of $a_{ij},\ j \in J_i$ is a symmetric bounded random parameter $\tilde{a}_{ij}$ (i.e., $a_{ij} \in [\tilde{a}_{ij} - \check{a}_{ij}, \tilde{a}_{ij} + \hat{a}_{ij}], \check{a}_{ij} = \hat{a}_{ij}$; $\boldsymbol{b}$ is the vector of upper bounds of the uncertain constraint (A.1b); $\boldsymbol{l}$ and $\boldsymbol{u}$ are the vectors of lower and upper bounds of the inequality constraint (A.1c), respectively.

In (A.1), it is assumed that uncertainty only affects matrix $\boldsymbol{A}$ in (A.1b) since if the uncertainty of objective function $\boldsymbol{c}$ needs to be modeled, it can be done by including the constraint $z - \boldsymbol{c}^\top \boldsymbol{x} \le 0$ into constraint (A.1b) and maximize the auxiliary objective function z.

Then, the non-linear formulation (A.2) is proposed as the RO of the problem (A.1).

$$\max \boldsymbol{c}^\top \boldsymbol{x} \,, \tag{A.2a}$$

st.

$$\sum_j \tilde{a}_{ij} x_j + \max_{\{S_i \cup \{h_i\} | S_i \subseteq J_i, |S_i| = \lfloor \Gamma_i \rfloor, h_i \in J_i \setminus S_i\}} \left\{ \sum_{j \in S_i} \check{a}_{ij} y_j + (\Gamma_i - \lfloor \Gamma_i \rfloor) \, \check{a}_{ih_i} y_h \right\} \le b_i \,, \qquad \forall i \tag{A.2b}$$

$$-y_j \le x_j \le y_j \,, \qquad \forall j \tag{A.2c}$$

$$\boldsymbol{l} \le \boldsymbol{x} \le \boldsymbol{u} \,, \tag{A.2d}$$

$$\boldsymbol{y} \ge 0 \,, \tag{A.2e}$$

where set S_i includes the optimization variables in problem (A.2b)-(A.2e) that correspond to the integer part of the uncertainty budget Γ_i ($\lfloor \Gamma_i \rfloor$) and is defined by a subset of the uncertainty set J_i; index h_i contains one optimization variable in problem (A.2b)-(A.2e) that corresponds to the non-integer remaining part of the uncertainty budget ($\Gamma_i - \lfloor \Gamma_i \rfloor$) and belongs to the uncertainty set J_i, while it is not contained in the set S_i; parameter Γ_i takes value in the interval $[0, |J_i|]$ and adjusts the level of robustness that the user chooses for the uncertainty.

Given the vector of optimal values $\boldsymbol{x}^*$, it is proved that the objective function of the linear problem (A.3) is equivalent to selecting the subset $\{S_i \cup \{h_i\} | S_i \subseteq J_i, |S_i| = \lfloor \Gamma_i \rfloor, h_i \in J_i \backslash S_i\}$ within the protection function of ith constraint (A.2b) (second term on the left-hand side of (A.2b)).

$$\beta_i(\boldsymbol{x}^*, \Gamma_i) = max \sum_{j \in J_i} \check{a}_{ij} \left| x_j^* \right| z_{ij} \, , \tag{A.3a}$$

st.

$$\sum_{j \in J_i} z_{ij} \leq \Gamma_i \, , \tag{A.3b}$$

$$0 \leq z_{ij} \leq 1 \, , \qquad \forall j \in J_i \tag{A.3c}$$

where x_j^* is the optimal value of the ith constraint; and z_{ij} is a positive variable less than 1.

Finally, by applying the strong duality theorem to (A.3) and substituting the result to the problem (A.2b)-(A.2e), the equivalent linear robust formulation is obtained as (A.4):

$$\max \boldsymbol{c}^\top \boldsymbol{x} \, , \tag{A.4a}$$

st.

$$\sum_j \tilde{a}_{ij} x_j + z_i \Gamma_i + \sum_{j \in J_i} p_{ij} \leq b_i \, , \qquad \forall i \tag{A.4b}$$

$$z_i + p_{ij} \geq \check{a}_{ij} y_j \, , \qquad \forall i, j \in J_i \tag{A.4c}$$

$$-y_j \leq x_j \leq y_j \, , \qquad \forall j \tag{A.4d}$$

$$l_j \leq x_j \leq u_j \, , \qquad \forall j \tag{A.4e}$$

$$p_{ij} \geq 0 \, , \qquad \forall i, j \in J_i \tag{A.4f}$$

$$y_j \geq 0 \, , \qquad \forall j \tag{A.4g}$$

$$z_i \geq 0 \, , \qquad \forall i \tag{A.4h}$$

where z_i and p_{ij} are dual variables of constraints (A.3b) and (A.3c), respectively; y_j is the auxiliary variable that calculates the x_j absolute value function; l_j and u_j are the elements of vectors $\boldsymbol{l}$ and $\boldsymbol{u}$, respectively.

The proposed model by Bertsimas and Sim in (A.4) is a linear optimization problem; however, it is shown in [27] that the proposed approach is also valid when the original problem is an MILP (i.e., when some of the variables in the vector $\boldsymbol{x}$ are integer), such as the problem proposed in this paper.

Appendix B. Asymmetric Robust Approach

The flexible RO approach with asymmetric uncertainty used in this paper is developed based on the symmetric RO model described in [27] (explained in Appendix A) and the forward-backward asymmetric RO model presented in [44]. To develop the flexible RO framework with asymmetric uncertainty, a similar procedure and proofs of feasibility and optimal solution are used as in [27] and [44], with some modifications. The main difference lies in the formulation of the protection function for uncertain parameters.

The asymmetric uncertainty model proposed in this paper represents a specific type of forward-backward asymmetric RO model as described in [44]. This distinction arises because the protection function in [44] is defined more generally for all possible conditions of the uncertain parameter and its associated variable. In defining the protection function, the two most important factors are the deviation of the uncertain parameter and the variable by which it is multiplied. For example, in the case of uncertainty in DAM electricity prices, the protection function needs to be formed based on the positive or negative deviations of the electricity price multiplied by the traded energy of the RVPP. The protection function defined in this paper takes into account the fact that, for example, the worst case of electricity price uncertainty occurs with a negative price deviation when the RVPP is an energy seller on the market and with a positive price deviation when the RVPP is an energy buyer.

To develop the asymmetric RO approach, consider the linear optimization problem (B.1):

$$\max\ \boldsymbol{c}^{\top}\boldsymbol{x}\,, \tag{B.1a}$$

st.

$$\boldsymbol{A}\boldsymbol{x} \leq \boldsymbol{b}\,, \tag{B.1b}$$

$$\boldsymbol{l} \leq \boldsymbol{x} \leq \boldsymbol{u}\,, \tag{B.1c}$$

Each entry of $a_{ij},\ j \in J_i$ in the matrix $\boldsymbol{A}$ is an asymmetric bounded random parameter $\tilde{a}_{ij}$ (i.e., $a_{ij}\in[\tilde{a}_{ij} - \check{a}_{ij}, \tilde{a}_{ij} + \hat{a}_{ij}], \check{a}_{ij} \neq \hat{a}_{ij}$). Other parameters and variables in (B.1) are defined similar to (A.1) in Appendix A.

For the asymmetric uncertainty set a_{ij}, unlike the symmetric uncertainty set, the protection function of the uncertain constraint changes not only based on the sign of the optimal value x_j^* but also based on the different deviations $\hat{a}_{ij}$ and $\check{a}_{ij}$. When the optimal value of x_j^* is negative, the worst case of the uncertain parameter a_{ij} occurs with positive deviation $\hat{a}_{ij}$, and accordingly the protection function is defined as (B.2a). For the positive value of x_j^*, the worst case occurs with negative deviation $\check{a}_{ij}$ and accordingly the protection function is defined as (B.2b).

$$\hat{\beta}(\boldsymbol{x}^*, \Gamma_i) = \max_{\{S_i\cup\{h_i\}|S_i\subseteq J_i, |S_i|=\lfloor\Gamma_i\rfloor, h_i\in J_i\setminus S_i\}} \left\{ \sum_{j\in S_i} \hat{a}_{ij} \left|x_j^*\right| + (\Gamma_i - \lfloor\Gamma_i\rfloor)\, \hat{a}_{ih_i} \left|x_j^*\right| \right\}, \qquad \forall i \tag{B.2a}$$

$$\check{\beta}(\boldsymbol{x}^*, \Gamma_i) = \max_{\{S_i\cup\{h_i\}|S_i\subseteq J_i, |S_i|=\lfloor\Gamma_i\rfloor, h_i\in J_i\setminus S_i\}} \left\{ \sum_{j\in S_i} \check{a}_{ij} \left|x_j^*\right| + (\Gamma_i - \lfloor\Gamma_i\rfloor)\, \check{a}_{ih_i} \left|x_j^*\right| \right\}, \qquad \forall i \tag{B.2b}$$

It is possible to write the protection functions (B.2a) and (B.2b) with only one protection function (B.3) that considers both conditions using a positive auxiliary variable y_j.

$$\beta(\boldsymbol{x}^*, \Gamma_i) = \max_{\{S_i\cup\{h_i\}|S_i\subseteq J_i, |S_i|=\lfloor\Gamma_i\rfloor, h_i\in J_i\setminus S_i\}} \left\{ \sum_{j\in S_i} \check{a}_{ij} y_j + (\Gamma_i - \lfloor\Gamma_i\rfloor)\, \check{a}_{ih_i} y_h \right\}, \qquad \forall i \tag{B.3a}$$

$$-\frac{\check{a}_{ij}}{\hat{a}_{ij}} y_j \leq x_j \leq y_j\,, \qquad \forall i, j \in J_j \tag{B.3b}$$

In (B.2a), since x_j^* is negative, the left side of (B.3b), i.e. $-\frac{\check{a}_{ij}}{\hat{a}_{ij}} y_j \leq x_j$ is active, so the expression $\frac{\check{a}_{ij}}{\hat{a}_{ij}} y_j$ (and correspondingly $\frac{\check{a}_{ih_i}}{\hat{a}_{ih_i}} y_h$) is substituted instead of $\left|x_j^*\right|$, which results in (B.3a). In (B.2b), since x_j^* is positive, the right side of (B.3b), i.e. $x_j \leq y_j$, is active, so the positive auxiliary variable y_j (and correspondingly y_h) is substituted instead of $\left|x_j^*\right|$, which results in (B.3a). Note that considering above explanation although (B.3a) includes only the negative deviation $\check{a}_{ij}$ (and correspondingly $\check{a}_{ih_i}$), it considers both positive and negative deviations of the asymmetric uncertain parameter through constraint (B.3b).

The protection function (B.3a) for the asymmetric uncertainty has the same structure as the protection function for the symmetric uncertainty in Appendix A and [27] (by considering also the constraint (B.3b)). Therefore, the same procedure and proof as for the symmetric uncertainty can be used here to obtain the robust formulation for the asymmetric uncertainty by considering a different limits as (B.3b) for the auxiliary variable y_j. The final asymmetric robust model is developed as in (B.4) by applying the strong duality theorem.

$$\max \boldsymbol{c}^\top \boldsymbol{x} \,, \tag{B.4a}$$

st.

$$\sum_j \tilde{a}_{ij} x_j + z_i \Gamma_i + \sum_{j \in J_i} p_{ij} \leq b_i \,, \qquad \forall i \tag{B.4b}$$

$$z_i + p_{ij} \geq \check{a}_{ij} y_j \,, \qquad \forall i, j \in J_i \tag{B.4c}$$

$$-\frac{\check{a}_{ij}}{\hat{a}_{ij}} y_j \leq x_j \leq y_j \,, \qquad \forall i, j \in J_i \tag{B.4d}$$

$$l_j \leq x_j \leq u_j \,, \qquad \forall j \tag{B.4e}$$

$$p_{ij} \geq 0 \,, \qquad \forall i, j \in J_i \tag{B.4f}$$

$$y_j \geq 0 \,, \qquad \forall j \tag{B.4g}$$

$$z_i \geq 0 \,, \qquad \forall i \tag{B.4h}$$

Appendix C. Sub-region Network Constraints

In this Appendix, the internal sub-region network of the RVPP, provided that the units in the portfolio are "electrically close" to each other and belong to a defined geographical sub-region, is formulated. The equations for a DC power flow used for active power trading in DAM and SRM are presented below. Note that, for IDMs participation, the time periods vary from $\forall t \in T$ to $\forall t \geq \tau$. The active power flow through transmission line l is represented in (C.1a), whereas the bounds of active power flow through transmission line l are imposed by (C.1b). Finally, the voltage angle reference and angle limits are set by (C.1c) and (C.1d), respectively.

$$p_{l,t} = (1/X_l)(\delta_{i(l),t} - \delta_{j(l),t}) \,, \qquad \forall l, t \tag{C.1a}$$

$$\underline{P}_l \leq p_{l,t} \leq \bar{P}_l \,, \qquad \forall l, t \tag{C.1b}$$

$$\delta_{b,t} = 0 \,, \qquad b : ref., \forall t \tag{C.1c}$$

$$-\pi \leq \delta_{b,t} \leq \pi \,, \qquad \forall b, t \tag{C.1d}$$

In the above constraints, $p_{l,t}$ is the active power flow through transmission line l in time period t. X_l is the reactance of transmission line l. $\delta_{b,t}$ is the voltage angle at bus b in time period t. $i(l)$ and $j(l)$ are sending and receiving bus of transmission line l, respectively. $\bar{P}_l$ is the capacity of transmission line l.

To implement the sub-region network constraints, the supply-demand balancing constraints for each market session defined in Section 4.2.1 are modified according to constraints (C.2)-(C.4). Constraints (C.2a) and (C.2b) enforce the supply-demand balancing for the RVPP units considering both energy and up/down SR in the DAM+SRM for the main sub-region buses ($\mathcal{B}_m$) and other buses ($\mathcal{B}/\mathcal{B}_m$), respectively.

$$\sum_{r\in\mathcal{R}}\left[p_{r,t}^{DA}+r_{r,t}^{SR}\right]+\sum_{\theta\in\Theta}\left[p_{\theta,t}^{DA}+r_{\theta,t}^{SR}\right]-\sum_{l|i(l)=b}p_{l,t}+\sum_{l|j(l)=b}p_{l,t}=p_t^{DA}+r_t^{SR}+\sum_{d\in\mathcal{D}}\left[p_{d,t}^{DA}-r_{d,t}^{SR}\right],\quad \forall b\in\mathcal{B}_m,\forall t \tag{C.2a}$$

$$\sum_{r\in\mathcal{R}}\left[p_{r,t}^{DA}+r_{r,t}^{SR}\right]+\sum_{\theta\in\Theta}\left[p_{\theta,t}^{DA}+r_{\theta,t}^{SR}\right]-\sum_{l|i(l)=b}p_{l,t}+\sum_{l|j(l)=b}p_{l,t}=\sum_{d\in\mathcal{D}}\left[p_{d,t}^{DA}-r_{d,t}^{SR}\right],\forall b\in\mathcal{B}/\mathcal{B}_m,\forall t \tag{C.2b}$$

The supply-demand balancing constraints in the SRM+IDM#1 for the main sub-region buses and other buses are formulated in (C.3a) and (C.3b), respectively.

$$\begin{aligned}&\sum_{r\in\mathcal{R}}\left[p_{r,t}^{DA^*}+p_{(k=1),r,t}^{ID}+r_{r,t}^{SR}\right]+\sum_{\theta\in\Theta}\left[p_{\theta,t}^{DA^*}+p_{(k=1),\theta,t}^{ID}+r_{\theta,t}^{SR}\right]\\&-\sum_{l|i(l)=b}p_{l,t}+\sum_{l|j(l)=b}p_{l,t}=p_t^{DA^*}+p_{(k=1),t}^{ID}+r_t^{SR}+\sum_{d\in\mathcal{D}}\left[p_{d,t}^{DA^*}+p_{(k=1),d,t}^{ID}-r_{d,t}^{SR}\right],\qquad \forall b\in\mathcal{B}_m,\forall t\end{aligned} \tag{C.3a}$$

$$\begin{aligned}&\sum_{r\in\mathcal{R}}\left[p_{r,t}^{DA^*}+p_{(k=1),r,t}^{ID}+r_{r,t}^{SR}\right]+\sum_{\theta\in\Theta}\left[p_{\theta,t}^{DA^*}+p_{(k=1),\theta,t}^{ID}+r_{\theta,t}^{SR}\right]\\&-\sum_{l|i(l)=b}p_{l,t}+\sum_{l|j(l)=b}p_{l,t}=\sum_{d\in\mathcal{D}}\left[p_{d,t}^{DA^*}+p_{(k=1),d,t}^{ID}-r_{d,t}^{SR}\right],\qquad \forall b\in\mathcal{B}/\mathcal{B}_m,\forall t\end{aligned} \tag{C.3b}$$

The supply-demand balancing constraints in the IDM#k for the main sub-region buses and other buses are formulated in (C.4a) and (C.4b), respectively.

$$\begin{aligned}&\sum_{r\in\mathcal{R}}\left[p_{r,t}^{DA^*}+r_{r,t}^{SR}+\sum_{k=1}^{k-1}p_{k,r,t}^{ID^*}+p_{k,r,t}^{ID}\right]+\sum_{\theta\in\Theta}\left[p_{\theta,t}^{DA^*}+r_{\theta,t}^{SR}+\sum_{k=1}^{k-1}p_{k,\theta,t}^{ID^*}+p_{k,\theta,t}^{ID}\right]-\sum_{l|i(l)=b}p_{l,t}\\&+\sum_{l|j(l)=b}p_{l,t}=p_t^{DA^*}+r_t^{SR^*}+\sum_{k=1}^{k-1}p_{k,t}^{ID^*}+p_{k,t}^{ID}+\sum_{d\in\mathcal{D}}\left[p_{d,t}^{DA^*}-r_{d,t}^{SR}+\sum_{k=1}^{k-1}p_{k,d,t}^{ID^*}+p_{k,d,t}^{ID}\right],\forall b\in\mathcal{B}_m,\forall k,t\geq\tau\end{aligned} \tag{C.4a}$$

$$\begin{aligned}&\sum_{r\in\mathcal{R}}\left[p_{r,t}^{DA^*}+r_{r,t}^{SR}+\sum_{k=1}^{k-1}p_{k,r,t}^{ID^*}+p_{k,r,t}^{ID}\right]+\sum_{\theta\in\Theta}\left[p_{\theta,t}^{DA^*}+r_{\theta,t}^{SR}+\sum_{k=1}^{k-1}p_{k,\theta,t}^{ID^*}+p_{k,\theta,t}^{ID}\right]-\sum_{l|i(l)=b}p_{l,t}\\&+\sum_{l|j(l)=b}p_{l,t}=\sum_{d\in\mathcal{D}}\left[p_{d,t}^{DA^*}-r_{d,t}^{SR}+\sum_{k=1}^{k-1}p_{k,d,t}^{ID^*}+p_{k,d,t}^{ID}\right],\qquad \forall b\in\mathcal{B}/\mathcal{B}_m,\forall k,t\geq\tau\end{aligned} \tag{C.4b}$$

Appendix D. Out-of-sample Assessment

In this Appendix, an out-of-sample assessment is presented to evaluate the performance of the proposed model compared to [28]. To reach this goal, a set of $|\omega|$ random scenarios with equal probability is generated for DAM and SRM electricity prices, available ND-RESs power production, thermal power output of the solar field of STUs, and demands. The corresponding parameters for each scenario are $\lambda^{DA}_{t,\omega}, \lambda^{SR,\uparrow}_{t,\omega}, \lambda^{SR,\downarrow}_{t,\omega}, P^{DA}_{r,t,\omega}, P^{DA}_{\theta,t,\omega}$, and $P^{DA}_{d,t,\omega}$, respectively. Then the scenario-based problem (D.1) is solved by using the generated scenarios for uncertain parameters and by fixing the obtained market bid results of solving the proposed model in (7), i.e. the energy and reserve bid variables $p^{DA^*}_t$, $r^{\mathrm{SR},\uparrow^*}_t$, and $r^{\mathrm{SR},\downarrow^*}_t$, as well as the variable of selection of load profiles $u^*_{d,p}$.

$$\max_{\Xi^{DA}} \frac{1}{|\omega|}\Bigg\{\sum_{\omega\in\Omega}\sum_{t\in\mathcal{T}}\Big[\lambda^{DA}_{t,\omega} p^{DA^*}_t \Delta t + \lambda^{SR,\uparrow}_{t,\omega} r^{\mathrm{SR},\uparrow^*}_t + \lambda^{\mathrm{SR},\downarrow}_{t,\omega} r^{\mathrm{SR},\downarrow^*}_t\Big]$$
$$- \sum_{\omega\in\Omega}\sum_{t\in\mathcal{T}}\sum_{r\in\mathcal{R}} C^R_r p^{DA}_{r,t,\omega}\Delta t - \sum_{d\in\mathcal{D}}\sum_{p\in\mathcal{P}} C_{d,p} u^*_{d,p} - \sum_{\omega\in\Omega}\sum_{t\in\mathcal{T}} Z\kappa_{t,\omega}\Delta t\Bigg\} \tag{D.1a}$$

st.

$$\sum_{r\in\mathcal{R}}\Big[p^{DA}_{r,t,\omega} + r^{SR}_{r,t,\omega}\Big] + \sum_{\theta\in\Theta}\Big[p^{DA}_{\theta,t,\omega} + r^{SR}_{\theta,t,\omega}\Big] = p^{DA^*}_t + r^{SR^*}_t - \kappa_{t,\omega} + \sum_{d\in\mathcal{D}}\Big[p^{DA}_{d,t,\omega} - r^{SR}_{d,t,\omega}\Big], \quad \forall\ t,\omega \tag{D.1b}$$
$$\underline{P}^{DA}_r \le p^{DA}_{r,t,\omega} - r^{SR,\downarrow}_{r,t,\omega}, \quad \forall r,t,\omega \tag{D.1c}$$
$$p^{DA}_{r,t,\omega} + r^{SR,\uparrow}_{r,t,\omega} \le P^{DA}_{r,t,\omega}, \quad \forall r,t,\omega \tag{D.1d}$$
$$0 \le p^{SF}_{\theta,t,\omega} \le P^{DA}_{\theta,t,\omega}, \quad \forall \theta,t,\omega \tag{D.1e}$$
$$p^{DA}_{d,t,\omega} = P^{DA}_{d,t,\omega}, \quad \forall d,t,\omega \tag{D.1f}$$
$$r^{SR,\uparrow}_{d,t,\omega} \le \underline{\beta}_{d,t}\sum_{p\in\mathcal{P}}\hat{P}_{d,p,t}u^*_{d,p}, \quad \forall d,t,\omega \tag{D.1g}$$
$$r^{SR,\uparrow}_{d,t,\omega} \le p^{DA}_{d,t,\omega} - \underline{P}_d, \quad \forall d,t,\omega \tag{D.1h}$$
$$r^{SR,\downarrow}_{d,t,\omega} \le \bar{\beta}_{d,t}\sum_{p\in\mathcal{P}}\hat{P}_{d,p,t}u^*_{d,p}, \quad \forall d,t,\omega \tag{D.1i}$$
$$r^{SR,\downarrow}_{d,t,\omega} \le \bar{P}_d - p^{DA}_{d,t,\omega}, \quad \forall d,t,\omega \tag{D.1j}$$
$$\Big(p^{DA}_{d,t,\omega} + r^{SR,\downarrow}_{d,t,\omega}\Big) - \Big(p^{DA}_{d,(t-1),\omega} - r^{SR,\uparrow}_{d,(t-1),\omega}\Big) \le \bar{R}_d\Delta t, \quad \forall d,t,\omega \tag{D.1k}$$
$$\Big(p^{DA}_{d,(t-1),\omega} + r^{SR,\downarrow}_{d,(t-1),\omega}\Big) - \Big(p^{DA}_{d,t,\omega} - r^{SR,\uparrow}_{d,t,\omega}\Big) \le \underline{R}_d\Delta t, \quad \forall d,t,\omega \tag{D.1l}$$
$$r^{SR,\uparrow}_{d,t,\omega} \le T^{SR}\underline{R}^{SR}_d, \quad \forall d,t,\omega \tag{D.1m}$$
$$r^{SR,\downarrow}_{d,t,\omega} \le T^{SR}\bar{R}^{SR}_d, \quad \forall d,t,\omega \tag{D.1n}$$
$$\underline{E}_d \le \sum_{t\in\mathcal{T}}\Big(p^{DA}_{d,t,\omega}\Delta t - r^{SR,\uparrow}_{d,t,\omega}\Big), \quad \forall d,\ \omega \tag{D.1o}$$

In problem (D.1), the variables $p^{DA}_{r,t,\omega}$, $r^{SR,\uparrow}_{r,t,\omega}$, $r^{SR,\downarrow}_{r,t,\omega}$, $r^{SR}_{r,t,\omega}$, $p^{DA}_{\theta,t,\omega}$, $p^{DA}_{d,t,\omega}$, $r^{SR,\uparrow}_{d,t,\omega}$, $r^{SR,\downarrow}_{d,t,\omega}$, and $r^{SR}_{d,t,\omega}$ related to power and reserve provided by ND-RESs, STUs, and demands are written for each scenario ω. The first three terms in the objective function (D.1a) calculate the operating profit of RVPP in all scenarios for DAM energy and SRM reserve participation, named by Π^{av}. The fourth term of (D.1a) determines the average penalization cost due to not providing some or whole part of energy bid in the market, named by K^{av}. The net profit of RVPP can be calculated as $\Pi^{av} - K^{av}$. The slack variable $\kappa_{t,\omega}$ is added in the supply-demand balancing constraint (D.1b) and is penalized by parameter Z in the objective function. Constraints (D.1c)-(D.1d) are scenario-based constraints for ND-RESs. Constraint (D.1e) is scenario-based constraint for STUs. Constraints (D.1f)-(D.1o) are scenario-based constraints for demands.

Appendix E. Weibull Probability Distribution Fitting

In this paper, the Weibull probability distribution fitting is used to generate scenarios for the out-of-sample assessment. Furthermore, the scenarios for the SP model [1] are generated based on the fitting of the Weibull probability distribution. While other probability distributions, such as the Log-normal, Gamma, Exponential, and Beta distributions [65], could be used to fit the historical data, the Weibull probability distribution has been demonstrated to provide an appropriate fit for various uncertain parameters, including DAM and SRM electricity prices, wind energy, STU thermal energy, and solar energy [65–68]. To validate the fitted distributions for various uncertain parameters, several tests, including the Kolmogorov-Smirnov (KS) Test, Mean Absolute Error (MAE), and Wasserstein Distance [69], are employed, as summarized in Table E1. These tests aim to compare the generated scenarios using the fitted Weibull distribution with the historical data. The results of these tests confirm that the fitted distributions are not significantly different from the original historical data. The fitted distributions for all uncertain parameters for a specific hour are also presented in Figure E1.

Table E1: Validation results of Weibull fitted distribution for uncertain parameters in a specific hour.

Test Name	Threshold	DAM Price	SRM Price	Wind Energy	STU Thermal Energy	Solar Energy
Kolmogorov-Smirnov (KS)	Test Statistic $D \leq 0.2$	0.1300	0.1533	0.1067	0.1367	0.0967
	P-value ≥ 0.05	0.8027	0.6129	0.9435	0.7506	0.9762
	Result	Not Different	Not Different	Not Different	Not Different	Not Different
Mean Absolute Error (MAE)	MAE ≤ 0.1	0.0639	0.0662	0.0327	0.0952	0.0874
Wasserstein Distance	Distance ≤ 2.0	1.7331	1.4713	0.8919	1.7883	1.2489

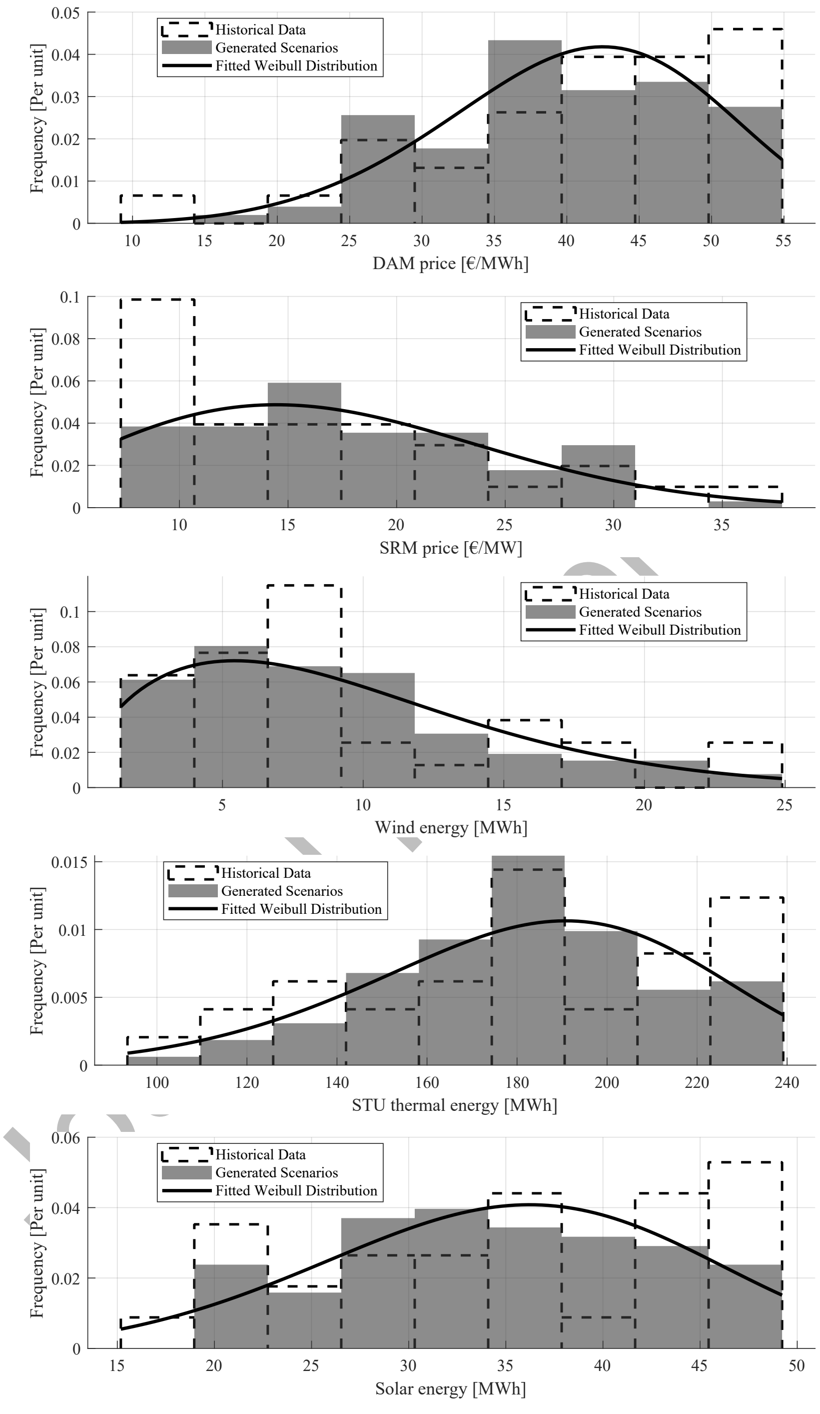

Figure E1: Historical data of uncertain parameters and associated bounds in a specific hour.

References

[1] L. Baringo, M. Rahimiyan, Virtual power plants and electricity markets: Decision making under uncertainty, Springer International Publishing, 2020.

[2] Á. Ortega, O. Oladimeji, H. Nemati, L. Sigrist, P. Sánchez-Martín, L. Rouco, E. Lobato, M. Biencinto, I. López, Modeling of VPPs for their optimal operation and configuration, Tech. rep., POSYTYF Consortium, deliverable 5.1. (2021).

[3] N. Naval, J. M. Yusta, Virtual power plant models and electricity markets-A review, Renewable and Sustainable Energy Reviews 149 (2021) 111393.

[4] A. F. Minai, A. A. Khan, K. Bahn, M. F. Ndiaye, T. Alam, R. Khargotra, T. Singh, Evolution and role of virtual power plants: Market strategy with integration of renewable based microgrids, Energy Strategy Reviews 53 (2024) 101390.

[5] D. Wozabal, G. Rameseder, Optimal bidding of a virtual power plant on the spanish day-ahead and intraday market for electricity, European Journal of Operational Research 280 (2) (2020) 639–655.

[6] I. Egido, F. Fernandez-Bernal, L. Rouco, The spanish AGC system: Description and analysis, IEEE Transactions on Power Systems 24 (1) (2009) 271–278.

[7] L. A. Roald, D. Pozo, A. Papavasiliou, D. K. Molzahn, J. Kazempour, A. Conejo, Power systems optimization under uncertainty: A review of methods and applications, Electric Power Systems Research 214 (2023) 108725.

[8] S. Yu, F. Fang, Y. Liu, J. Liu, Uncertainties of virtual power plant: Problems and countermeasures, Applied energy 239 (2019) 454–470.

[9] J. F. Venegas-Zarama, J. I. Muñoz-Hernandez, L. Baringo, P. Diaz-Cachinero, I. De Domingo-Mondejar, A review of the evolution and main roles of virtual power plants as key stakeholders in power systems, IEEE Access 10 (2022) 47937–47964.

[10] E. L. Miguélez, I. E. Cortés, L. R. Rodríguez, G. L. Camino, An overview of ancillary services in spain, Electric Power Systems Research 78 (3) (2008) 515–523.

[11] H. Khaloie, M. Mollahassani-Pour, A. Anvari-Moghaddam, Optimal behavior of a hybrid power producer in day-ahead and intraday markets: A bi-objective CVaR-based approach, IEEE Transactions on Sustainable Energy 12 (2) (2020) 931–943.

[12] R. M. Lima, A. J. Conejo, S. Langodan, I. Hoteit, O. M. Knio, Risk-averse formulations and methods for a virtual power plant, Computers & Operations Research 96 (2018) 350–373.

[13] X. Kong, J. Xiao, D. Liu, J. Wu, C. Wang, Y. Shen, Robust stochastic optimal dispatching method of multi-energy virtual power plant considering multiple uncertainties, Applied Energy 279 (2020) 115707.

[14] L. Ju, R. Zhao, Q. Tan, Y. Lu, Q. Tan, W. Wang, A multi-objective robust scheduling model and solution algorithm for a novel virtual power plant connected with power-to-gas and gas storage tank considering uncertainty and demand response, Applied Energy 250 (2019) 1336–1355.

[15] H. Wang, S. Riaz, P. Mancarella, Integrated techno-economic modeling, flexibility analysis, and business case assessment of an urban virtual power plant with multi-market co-optimization, Applied Energy 259 (2020) 114142.

[16] H. Nezamabadi, M. Setayesh Nazar, Arbitrage strategy of virtual power plants in energy, spinning reserve and reactive power markets, IET Generation, Transmission & Distribution 10 (3) (2016) 750–763.

[17] E. Mashhour, S. M. Moghaddas-Tafreshi, Bidding strategy of virtual power plant for participating in energy and spinning reserve markets—part I: Problem formulation, IEEE Transactions on Power Systems 26 (2) (2010) 949–956.

[18] L. Ju, Q. Tan, Y. Lu, Z. Tan, Y. Zhang, Q. Tan, A CVaR-robust-based multi-objective optimization model and three-stage solution algorithm for a virtual power plant considering uncertainties and carbon emission allowances, International Journal of Electrical Power & Energy Systems 107 (2019) 628–643.

[19] Y. Zhang, F. Liu, Z. Wang, Y. Su, W. Wang, S. Feng, Robust scheduling of virtual power plant under exogenous and endogenous uncertainties, IEEE Transactions on Power Systems 37 (2) (2021) 1311–1325.

[20] V. Singh, T. Moger, D. Jena, Uncertainty handling techniques in power systems: A critical review, Electric Power Systems Research 203 (2022) 107633.

[21] A. J. Conejo, M. Carrión, J. M. Morales, et al., Decision making under uncertainty in electricity markets, Vol. 1, Springer, 2010.

[22] P. Shinde, I. Kouveliotis-Lysikatos, M. Amelin, Multistage stochastic programming for VPP trading in continuous intraday electricity markets, IEEE Transactions on Sustainable Energy 13 (2) (2022) 1037–1048.

[23] M. Vahedipour-Dahraie, H. Rashidizadeh-Kermani, M. Shafie-Khah, J. P. Catalão, Risk-averse optimal energy and reserve scheduling for virtual power plants incorporating demand response programs, IEEE Transactions on Smart Grid 12 (2) (2020) 1405–1415.

[24] A. G. Zamani, A. Zakariazadeh, S. Jadid, Day-ahead resource scheduling of a renewable energy based virtual power plant, Applied Energy 169 (2016) 324–340.

[25] Y. Zhang, J. Chen, Y. Wang, L. Feng, Enhancing resilience of agricultural microgrid through electricity–heat–water based multi-energy hub considering irradiation intensity uncertainty, Renewable Energy 220 (2024) 119739.

[26] Y. Li, Q. Wu, M. Li, J. Zhan, Mean-variance model for power system economic dispatch with wind power integrated, Energy 72 (2014) 510–520.

[27] D. Bertsimas, M. Sim, The price of robustness, Operations Research 52 (1) (2004) 35–53.

[28] M. Rahimiyan, L. Baringo, Strategic bidding for a virtual power plant in the day-ahead and real-time markets: A price-taker robust optimization approach, IEEE Transactions on Power Systems 31 (4) (2015) 2676–2687.

[29] A. A. Bafrani, A. Rezazade, M. Sedighizadeh, Robust electrical reserve and energy scheduling of power system considering hydro pumped storage units and renewable energy resources, Journal of Energy Storage 54 (2022) 105310.

[30] Y. Li, Q. Wu, L. Jiang, J.-B. Yang, D.-L. Xu, Optimal power system dispatch with wind power integrated using nonlinear interval optimization and evidential reasoning approach, IEEE Transactions on Power Systems 31 (3) (2015) 2246–2254.

[31] J. Hu, C. Jiang, Y. Liu, Short-term bidding strategy for a price-maker virtual power plant based on interval optimization, Energies (Basel) 12 (19) (2019).

[32] Y. Liu, M. Li, H. Lian, X. Tang, C. Liu, C. Jiang, Optimal dispatch of virtual power plant using interval and deterministic combined optimization, International Journal of Electrical Power & Energy Systems 102 (2018) 235–244.

[33] A. T. Al-Awami, N. A. Amleh, A. M. Muqbel, Optimal demand response bidding and pricing mechanism with fuzzy optimization: Application for a virtual power plant, IEEE Transactions on Industry Applications 53 (5) (2017) 5051–5061.

[34] L. Ju, H. Li, J. Zhao, K. Chen, Q. Tan, Z. Tan, Multi-objective stochastic scheduling optimization model for connecting a virtual power plant to wind-photovoltaic-electric vehicles considering uncertainties and demand response, Energy Conversion and Management 128 (2016) 160–177.

[35] A. Baringo, L. Baringo, A stochastic adaptive robust optimization approach for the offering strategy of a virtual power plant, IEEE transactions on power systems 32 (5) (2016) 3492–3504.

[36] A. Baringo, L. Baringo, J. M. Arroyo, Day-ahead self-scheduling of a virtual power plant in energy and reserve electricity markets under uncertainty, IEEE Transactions on Power Systems 34 (3) (2018) 1881–1894.

[37] Z. Yuanyuan, Z. Huiru, L. Bingkang, Distributionally robust comprehensive declaration strategy of virtual power plant participating in the power market considering flexible ramping product and uncertainties, Applied Energy 343 (2023) 121133.

[38] S. Babaei, C. Zhao, L. Fan, A data-driven model of virtual power plants in day-ahead unit commitment, IEEE Transactions on Power Systems 34 (6) (2019) 5125–5135.

[39] S. Yu, F. Fang, J. Liu, Flexible operation of a CHP-VPP considering the coordination of supply and demand based on a strengthened distributionally robust optimization, IET Control Theory & Applications 17 (16) (2023) 2146–2161.

[40] H. Liu, J. Qiu, J. Zhao, A data-driven scheduling model of virtual power plant using wasserstein distributionally robust optimization, International Journal of Electrical Power & Energy Systems 137 (2022) 107801.

[41] M. Khojasteh, P. Faria, F. Lezama, Z. Vale, A novel adaptive robust model for scheduling distributed energy resources in local electricity and flexibility markets, Applied Energy 342 (2023) 121144.

[42] Z. Li, M. Liu, M. Xie, J. Zhu, Robust optimization approach with acceleration strategies to aggregate an active distribution system as a virtual power plant, International Journal of Electrical Power & Energy Systems 142 (2022) 108316.

[43] G. K. Sakki, I. Tsoukalas, P. Kossieris, C. Makropoulos, A. Efstratiadis, Stochastic simulation-optimization framework for the design and assessment of renewable energy systems under uncertainty, Renewable and Sustainable Energy Reviews 168 (2022) 112886.

[44] X. Chen, M. Sim, P. Sun, A robust optimization perspective on stochastic programming, Operations research 55 (6) (2007) 1058–1071.

[45] S.-C. Kang, Robust linear optimization using distributional information, ProQuest, 2008.

[46] G. Wang, Q. Bian, H. Xin, Z. Wang, A robust reserve scheduling method considering asymmetrical wind power distribution, IEEE/CAA Journal of Automatica Sinica 5 (5) (2017) 961–967.

[47] S.-C. Kang, T. S. Brisimi, I. C. Paschalidis, Distribution-dependent robust linear optimization with applications to inventory control, Annals of operations research 231 (1) (2015) 229–263.

[48] C. Büsing, F. D'andreagiovanni, New results about multi-band uncertainty in robust optimization, in: International symposium on experimental algorithms, Springer, 2012, pp. 63–74.

[49] J. Li, S. Zhou, Y. Xu, M. Zhu, L. Ye, A multi-band uncertainty set robust method for unit commitment with wind power generation, International Journal of Electrical Power & Energy Systems 131 (2021) 107125.

[50] B. Hu, L. Wu, Robust SCUC with multi-band nodal load uncertainty set, IEEE Transactions on Power Systems 31 (3) (2015) 2491–2492.

[51] C. Dai, L. Wu, H. Wu, A multi-band uncertainty set based robust SCUC with spatial and temporal budget constraints, IEEE Transactions on Power Systems 31 (6) (2016) 4988–5000.

[52] C. Dai, L. Wu, A two-stage robust transmission expansion planning approach with multi-band uncertainty set, in: 2016 IEEE Power and Energy Society General Meeting (PESGM), IEEE, 2016, pp. 1–5.

[53] P. González, J. Villar, C. A. Díaz, F. A. Campos, Joint energy and reserve markets: Current implementations and modeling trends, Electric Power Systems Research 109 (2014) 101–111.

[54] O. Oladimeji, Á. Ortega, L. Sigrist, L. Rouco, P. Sánchez-Martín, E. Lobato, Optimal participation of heterogeneous, RES-based virtual power plants in energy markets, Energies 15 (9) (2022) 3207.

[55] Y. Chen, Y. Niu, M. Du, J. Wang, A two-stage robust optimization model for a virtual power plant considering responsiveness-based electric vehicle aggregation, Journal of Cleaner Production 405 (2023) 136690.

[56] G. Morales-España, Á. Lorca, M. M. de Weerdt, Robust unit commitment with dispatchable wind power, Electric Power Systems Research 155 (2018) 58–66.

[57] O. Oladimeji, A. Ortega, L. Sigrist, P. Sánchez-Martín, E. Lobato, L. Rouco, Modeling demand flexibility of RES-based virtual power plants, in: 2022 IEEE Power & Energy Society General Meeting (PESGM), IEEE, 2022, pp. 1–5.

[58] I. L. García, J. L. Álvarez, D. Blanco, Performance model for parabolic trough solar thermal power plants with thermal storage: Comparison to operating plant data, Solar Energy 85 (10) (2011) 2443–2460.

[59] J. Wang, Z. Hu, S. Xie, Expansion planning model of multi-energy system with the integration of active distribution network, Applied Energy 253 (2019) 113517.

[60] A. Srinivasan, R. Wu, P. Heer, G. Sansavini, Impact of forecast uncertainty and electricity markets on the flexibility provision and economic performance of highly-decarbonized multi-energy systems, Applied Energy 338 (2023) 120825.

[61] Y. Wen, D. AlHakeem, P. Mandal, S. Chakraborty, Y.-K. Wu, T. Senjyu, S. Paudyal, T.-L. Tseng, Performance evaluation of probabilistic methods based on bootstrap and quantile regression to quantify PV power point forecast uncertainty, IEEE transactions on neural networks and learning systems 31 (4) (2019) 1134–1144.

[62] Red Eléctrica de España, Electricity price forecast.
URL https://www.esios.ree.es/en/analysis/600

[63] Red Eléctrica de España, Measured wind geneartion.
URL https://www.esios.ree.es/en/analysis/10037

[64] M. Biencinto, L. González, L. Valenzuela, Using time-windowed solar radiation profiles to assess the daily uncertainty of solar thermal electricity production forecasts, Journal of Cleaner Production 379 (2022) 134821.

[65] G. Varathan, et al., A review of uncertainty management approaches for active distribution system planning, Renewable and Sustainable Energy Reviews 205 (2024) 114808.

[66] L. Ramirez-Burgueno, Y. Sang, Y. Zheng, Pricing wind power uncertainty in the electricity market, IEEE Access 11 (2023) 58624–58633.

[67] A. Mirzapour-Kamanaj, A. Talebi, K. Zare, B. Mohammadi-Ivatloo, Z. Abdul-Malek, A. Anvari-Moghaddam, Optimal look-ahead strategic bidding/offering of integrated renewable power plants and caes with stochastic-robust approach, IEEE Access 10 (2022) 107901–107912.

[68] A. K. ALAhmad, R. Verayiah, A. Ramasamy, M. Marsadek, H. Shareef, Optimal planning of energy storage system for hybrid power system considering multi correlated input stochastic variables, Journal of Energy Storage 82 (2024) 110615.

[69] S. Ncwane, K. A. Folly, Modeling wind speed using parametric and non-parametric distribution functions, IEEE Access 9 (2021) 104501–104512.

Declaration of interests

☒ The authors declare that they have no known competing financial interests or personal relationships that could have appeared to influence the work reported in this paper.

☐ The authors declare the following financial interests/personal relationships which may be considered as potential competing interests: